

FLORIDA STATE UNIVERSITY  
FAMU-FSU COLLEGE OF ENGINEERING

MECHANICAL PROPERTIES OF SUPERPOWER AND SUNAM  
REBCO COATED CONDUCTORS

By

KYLE RADCLIFF

A Thesis submitted to the  
Department of Mechanical Engineering  
in partial fulfillment of the  
requirements for the degree of  
Master of Science

2018

Copyright © 2018 Kyle Radcliff. All Rights Reserved.

Kyle Radcliff defended this thesis on November 15, 2018.  
The members of the supervisory committee were:

Seungyong Hahn  
Professor Directing Thesis

David C. LARBALÉSTIER  
Committee Member

Lance D. Cooley  
Committee Member

The Graduate School has verified and approved the above-named committee members, and certifies that the thesis has been approved in accordance with university requirements.

# ACKNOWLEDGMENTS

I would express the utmost gratitude to my academic advisor Dr. Seungyong Hahn for giving me the wonderful opportunity to pursue this research and for his continued support. I would also like to thank Dr. Lance D. Cooley for serving on my committee and offering his insight. Lastly, I want to thank Dr. David C. Larbalestier for acting as my co-advisor and sharing his wealth of knowledge and expertise. I am particularly grateful for Robert P. Walsh for welcoming me into his lab and providing access to his extensive low temperature mechanical property test setups and for guiding me to understand materials testing.

I also want to give a special thank you to the No-Insulation REBCO team at the National High Magnetic Field Laboratory: Kwang Lok Kim, Kwangmin Kim, Kabindra Bhattarai, and Xinbo Hu, for their continued support.

This work is supported by the National Science Foundation under grant number DMR- 1644779, the State of Florida, and the Korean Science Basic Institute grant (D38611) to SangGap Lee.

# TABLE OF CONTENTS

List of Tables . . . . .	vi
List of Figures . . . . .	vii
List of Symbols . . . . .	x
List of Abbreviations . . . . .	xi
Abstract . . . . .	xii
<b>1 Introduction</b>	<b>1</b>
1.1 Motivation . . . . .	1
1.2 Goals and Approach . . . . .	1
1.3 Introduction to REBCO Coated Conductor . . . . .	2
1.4 Types of REBCO Coated Conductor . . . . .	2
1.4.1 SuNAM REBCO CC . . . . .	3
1.4.2 SuperPower REBCO CC . . . . .	4
1.5 Introduction to Mechanics . . . . .	5
1.5.1 Engineering Stress and Strain . . . . .	5
1.5.2 Stress and Strain in Solenoid Magnets . . . . .	7
1.6 Defining Critical Current . . . . .	8
1.7 Literature Review . . . . .	9
1.7.1 ASTM Standards & Guidelines . . . . .	9
1.7.2 SuperPower REBCO CC vs. Copper Thickness . . . . .	9
<b>2 Experimental Procedures</b>	<b>11</b>
2.1 Tensile Testing . . . . .	11
2.1.1 Tension Machine . . . . .	11
2.1.2 Strain Gages . . . . .	12
2.1.3 Extensometer . . . . .	13
2.2 Sample Preparation . . . . .	14
2.2.1 Dimensions of REBCO CC . . . . .	14
2.2.2 Uncertainty Analysis . . . . .	16
2.2.3 Mounting REBCO CC . . . . .	17
2.3 Tensile Test Procedure . . . . .	18
2.4 Critical Current vs Strain Test Procedure . . . . .	19
<b>3 Results</b>	<b>20</b>
3.1 Stress-Strain Dependence on Different Batches SuNAM REBCO CC . . . . .	20
3.1.1 Batch 1 Fabricated July 29, 2016 . . . . .	20
3.1.2 Batch 2 Fabricated August 4, 2016 . . . . .	21
3.1.3 Batch 3 Fabricated on August 19,2016 . . . . .	22
3.2 Simulated Heat Treatment Effects of the REBCO Deposition Process on Hastelloy <sup>®</sup> and 310 SS Substrates . . . . .	23

3.2.1	As Received Condition . . . . .	24
3.2.2	Effects of 700 °C Heat Treatment . . . . .	25
3.2.3	Effects of 750 °C Heat Treatment . . . . .	26
3.2.4	Effects of 800 °C Heat Treatment . . . . .	27
3.3	$I_c$ -Strain Dependence of Different Batches on SuNAM REBCO CC . . . . .	27
3.3.1	Batch 1 Fabricated July 29, 2016 . . . . .	28
3.3.2	Batch 2 Fabricated August 4, 2016 . . . . .	29
3.3.3	Batch 3 Fabricated August 19, 2016 . . . . .	30
<b>4</b>	<b>Discussion</b>	<b>32</b>
4.1	Stress-Strain Variability of SuNAM REBCO CC . . . . .	32
4.2	Annealing Effects on Hastelloy <sup>®</sup> and 310 SS Substrates . . . . .	34
4.3	$I_c$ -Strain Dependence of SuNAM REBCO CC . . . . .	36
4.3.1	Slit Edge Effects on $I_c$ vs. Strain . . . . .	37
4.3.2	Strain Gage Reinforcement Effect . . . . .	37
<b>5</b>	<b>Conclusion</b>	<b>40</b>
<b>Appendix</b>		
<b>A</b>	<b>Dimensions of Measured Samples</b>	<b>41</b>
A.1	Dimensions of SuNAM REBCO CC . . . . .	41
References . . . . .		44
Biographical Sketch . . . . .		46

# LIST OF TABLES

2.1	Variation of conductor thickness and width of SuNAM CC . . . . .	16
3.1	Table of summarized results for the range and average $\sigma_{0.2}$ . . . . .	23
A.1	Dimensions of SuNAM REBCO CC Batch 1 . . . . .	41
A.2	Dimensions of SuNAM REBCO CC Batch 2 . . . . .	42
A.3	Dimensions of SuNAM REBCO CC Batch 3 . . . . .	43

# LIST OF FIGURES

1.1	Visual representation of SuNAM CC manufacturing process using reactive co-evaporation by deposition & reaction [2]. . . . .	3
1.2	Diagram of SuNAM REBCO CC with individual layer thickness [2]. . . . .	4
1.3	Diagram of SuperPower CC with individual layer thickness [3]. . . . .	4
1.4	Schematic representation of uniaxial tension on a specimen with a change of length and diameter [5]. . . . .	5
1.5	Linear elastic region of a stress-strain curve with the slope of the line defining elastic modulus E. [5]. . . . .	6
1.6	Stress vs. Strain curve with 0.2 yield strength offset, elastic and plastic regions, and approximately where the proportional limit is located [5]. . . . .	7
1.7	Representation of hoop stress in a solenoid magnet equating to uniaxial tension when the REBCO CC is wound along its neutral axis. . . . .	7
1.8	Voltage (V) vs. current (I) curve displaying the critical voltage and its corresponding critical current. . . . .	8
1.9	SuperPower REBCO CC stress vs. strain curves with each tape having 50 microns of Hastelloy <sup>®</sup> and varying copper thickness coated on each side of the conductor. Bare tape in this case indicates REBCO conductor without any copper stabilizer [9]. . . . .	9
1.10	SuperPower REBCO CC critical vs. strain curves with each tape having 50 microns of Hastelloy <sup>®</sup> and varying copper thickness at 77 K [9]. . . . .	10
2.1	Schematic representation of a universal tension testing machine [5]. . . . .	11
2.2	Graphical representative of a uniformed wire changing shape uniformly, altering its internal resistance. . . . .	12
2.3	Strain gage schematic showing the direction along which the gage can measure strain, and the resistance wires whose change in resistance when deformed determines the strain value [11]. . . . .	13
2.4	Two-inch Shepic extensometer with a side view (a) and knife edge shape (b). . . . .	14
2.5	Cross-sectional view of SuNAM REBCO CC with 100 microns of 310 SS and 7.5 microns of copper on each side. . . . .	15

2.6	Schematic diagram of how sample dimensions are taken where tape length is in the x-direction and the width is in the y-direction. Dots represent points where the thickness is taken, while arrows show where the points the width is taken. . . . .	15
2.7	Mounting grip for (a) tensile test and (b) $I_c$ vs. strain test. . . . .	17
2.8	Final mounting of REBCO CC for tensile tests. . . . .	18
2.9	Critical current vs strain mount inside a tension machine. Red circles indicate voltage taps placement, sample location, and current leads locations from the power supply. .	19
3.1	Stress vs. strain of SuNAM REBCO CC manufactured on July 29 <sup>th</sup> , 2016 (160729). Symbols do not represent the number of data points taken. Like symbols (i.e., squares, circles, and triangles) indicate different acquired taken from the same spool. Legend reads as follows, 160729-X-X: manufactured date-spool number-sample number. . . .	20
3.2	Stress vs. strain of SuNAM REBCO CC manufactured on August 4 <sup>th</sup> , 2016 (160804). Symbols do not represent the number of data points taken. Like symbols (i.e., squares, circles, and triangles) indicate different samples taken from the same spool. Legend reads as follows, 160804-X-X: manufactured date-spool number-sample number. . . .	21
3.3	Stress vs. strain of SuNAM REBCO CC manufactured on August 19 <sup>th</sup> , 2016 (160819). Symbols do not represent the number of data points taken. Like symbols (i.e., squares, circles, and triangles) indicate different samples taken from the same spool. Legend reads as follows, 160819-X-X: manufactured date-spool number-sample number. . . .	22
3.4	Temperature profiles of the simulated REBCO deposition heat treatments at 700, 750, and 800 °C. . . . .	23
3.5	Stress-strain dependence on as received Hastelloy <sup>®</sup> and 310 stainless steel, where 310SS-1 represents the type and sample number of the steel substrate tested, and H represents Hastelloy <sup>®</sup> with -8 indicating sample number. Test was performed at room temperature . . . . .	24
3.6	Effect of 700 °C simulated vapor deposition heat treatment Hastelloy and 310 stainless steel bare substrate. . . . .	25
3.7	Effect of 750 °C simulated REBCO deposition heat treatment on bare Hastelloy and 310 stainless steel substrates. . . . .	26
3.8	Effect of 800 °C simulated REBCO deposition heat treatment on bare Hastelloy and 310 stainless steel substrates. . . . .	27
3.9	Normalized critical current vs. strain of SuNAM CC batch 1 (160729). Closed symbols represent the critical current while the sample was under load and open symbols show the critical current at the no-load condition after the strain was applied at 77 K. . . .	28

3.10	Normalized critical current vs. strain of SuNAM CC batch 2. Closed symbols represent the critical current while the sample is under load and open symbols show the critical current at the no-load condition after the strain was applied at 77 K. Strain from samples 160804-02-5 and 160804-02-7 strain was measured using a one-inch clip-on extensometer. . . . .	29
3.11	Normalized critical current vs. strain of SuNAM CC batch 3. Closed symbols represent the critical current while the sample is under load and open symbols show the critical current at the no-load condition after the strain was applied at 77 K. . . . .	30
4.1	Stress vs. strain of 18 different SuNAM REBCO CC at 77 K, manufactured on August 19th, 2016 (160819), August 4th, 2016 (160804), and July 29th, 2016 (160729). I.e., 160819-4-1 represents manufactured date-spool number-sample number. . . . .	32
4.2	Thicknesses of layers in SuNAM REBCO CC (not to scale). Total copper thickness is 15 $\mu\text{m}$ , 1-1.5 $\mu\text{m}$ of REBCO, and 100 $\mu\text{m}$ of 310 SS. . . . .	33
4.3	Load vs. strain of the 18 SuNAM REBCO CC samples. Group (A) and (B) show "identical" conductors having different stiffnesses. . . . .	33
4.4	The average trend of as received and heat treated Hastelloy <sup>®</sup> C-276 and 310 SS bare substrate stress vs. strain curves at various conditions of heat treatments at AR(as received), 700°C, 750°C, and 800°C. . . . .	34
4.5	0.2 % yield strength vs. heat treatment on Hastelloy <sup>®</sup> C-276 (red circle) and 310 SS (black square) . . . . .	35
4.6	$I_c$ vs. strain of SuNAM REBCO CC. Solid symbols indicate $I'_c$ at strain, and open symbols indicate $I'_c$ after the strain was applied. The red box show tests done with a one-inch Shepic extensometer to ensure extensometers can be used in $I_c$ vs. strain tests. 36	36
4.7	$I_c$ vs. strain of SuNAM REBCO CC showing current dependence on strain. Labels indicate the type of slit edge on tested samples. . . . .	37
4.8	REBCO CC with a mounted strain gage. . . . .	38
4.9	Strain gage reinforcement is shown in a tensile test with extensometer as a cross check. Red dash is reading directly from strain gage, blue dash line is corrected for reinforcement effect, and the solid line shows the results from the extensometer. . . .	38

# LIST OF SYMBOLS

$\sigma$	Stress, MPa
$\epsilon$	Strain, $\frac{mm}{mm}$
$E$	Elastic Modulus, GPa
$V_c$	Critical Voltage, V
$I_c$	Critical Current, A
$K$	Kelvin, K
$\epsilon_c$	Critical Strain, $\frac{mm}{mm}$
$\epsilon_{irr}$	Irreversible Strain, $\frac{mm}{mm}$
$E_{eg}$	Equivalent Elastic Modulus, GPa
$E_u$	Unload Elastic Modulus, GPa
$E_o$	Initial Elastic Modulus, GPa
$\sigma_{y,0.2}$	0.2 % Yield Strength, MPa

# LIST OF ABBREVIATIONS

ASTM	“American Society for Testing and Materials”
CC	“Coated Conductor”
GF	“Gage Factor”
GL	“Gage Length”
HTS	“High Temperature Superconductor”
IBAD	“Ion Beam Assisted Deposition”
LTS	“Low Temperature Superconductor”
MOCVD	“Metalorganic Chemical Vapor Deposition”
NHMFL	“National High Magnetic Field Laboratory”
NI	”No-Insulation”
REBCO	“Rare Earth Barium Copper Oxide: $REBa_2Cu_3O_x$ ”
RCE-CDR	“Reactive co-evaporation by deposition & reaction”
SS	“Stainless Steel”

# ABSTRACT

High Temperature Superconductors (HTS) are the only practical way to achieve fields with superconducting magnets higher than the 25 T limit of Low Temperature Superconductors (LTS). No-Insulation (NI) REBCO magnets using REBa<sub>2</sub>Cu<sub>3</sub>O<sub>x</sub> as the superconductor require less copper stabilizer than insulated magnets and thin (30 μm) substrates have now become available. In our recent small coil attack on fields greater than 40 T, we have seen that overstrain damage can easily occur even at the frequently used design strain of 0.4%. Here we present an experimental study of the uniaxial stress ( $\sigma$ ) characteristics of SuperPower and SuNAM coated conductors and also do strain-critical current ( $I_c(\epsilon)$ ) measurements to find the onset of permanent damage to  $I_c$ . We found considerable variation in their 77 K mechanical properties. The cold-rolled Hastelloy C-276 substrate used by SuperPower is much stronger than the cold-rolled 310 stainless steel substrate used by SuNAM, but of more concern is the inconsistency of the strength of different batches of SuNAM tape. Mechanical variability in the different SuNAM batches creates a challenge when designing for magnets. We also examined the effects of strain on critical current performance, finding that the critical current degradation of the SuNAM conductor becomes irreversible over a wide range of strains from 0.3-0.6%. Suspecting that some annealing of the substrates occurs during REBCO deposition in the vicinity of 750 °C, we performed short heat treatments at 700, 750, and 800 °C on samples of the as-delivered substrates used by manufacturers. We found that there was little change to the strength of the Hastelloy used by SuperPower, but substantial change to the 310 stainless steel used by SuNAM. Our results show that any high field operation at strains of 0.4% or more requires detailed knowledge of the mechanical properties of the tapes being used, especially for magnets using SuNAM tapes with cold-rolled 310 stainless steel substrates.

# CHAPTER 1

## INTRODUCTION

### 1.1 Motivation

High field magnets made of REBCO coated conductor (CC) are thought by many to be the future route to ultra-high field superconducting magnets. However, the stresses produced in such magnets can be enormous. At the National High Field Laboratory (NHMFL), many of our future magnet designs are clearly stress/strain limited, placing great importance on understanding the strain limitations, presently thought to be  $\sim 0.4\%$ . This limit is set to establish safe working stresses that the REBCO CC can handle without suffering from degradation. It was found in this study, and various other studies that strains near  $0.4\%$  and  $0.5\%$  significantly affect the conductor properties.

This thesis primarily focuses on the SuNAM REBCO CC electro-mechanical properties, particularly stress-strain, and  $I_c$ -strain properties of SuNAM REBCO CC. A comparison of SuNAM and SuperPower REBCO CC is also made in this study. As we will find out in later chapters, the choice of metal substrate each company uses plays a crucial role. A better understanding of SuNAM REBCO CC may allow for a reduction in cost of high field magnets due to their faster and cheaper manufacturing process, as compared to SuperPower.

### 1.2 Goals and Approach

This thesis is aimed to characterize the factors and variables that contribute to the performance of REBCO CC. In particular, tensile stress ( $\sigma$ ) and critical current ( $I_c$ ) as a function of strain tests are done to gauge the performance of the REBCO CC. This becomes quite important for future magnet designs, especially when REBCO CC manufacturers have slightly different processes to produce their conductor.

Tensile and  $I_c$  vs. strain test procedures are quite similar. They both start with precise measurements of the conductor dimensions. The tensile test uses stainless steel grips with sandpaper

to ensure no slipping occurs while testing. Then, the sample is placed into an universal servo-hydraulic tension machine that will apply uniaxial tension in the sample.  $I_c$  vs. strain tests use copper grips embedded with tinned REBCO CC to promote current transfer into the sample. In incremental steps, strain is applied and critical current is then measured in a bath of liquid nitrogen at 77 K. After the samples are returned to a no-load condition, and critical current is measured once again until the sample can no longer carry current.

### 1.3 Introduction to REBCO Coated Conductor

High temperature superconductors (HTS) are believed to be the future for high field magnets  $> 25$  T. In 1987, the discovery of  $\text{YBa}_2\text{Cu}_3\text{O}_{7-x}$  (YBCO), or more generally  $(\text{RE})\text{Ba}_2\text{Cu}_3\text{O}_x$  (REBCO), having a critical temperature of about 93 K, thus superconducting at 77 K [1], paved the way for superconducting applications without having to operate in a bath of liquid helium at 4.2 K. This offers a cheaper alternative for cooling and the potential for higher fields over a wide range of temperatures. REBCO CC is intentionally made as thin as possible to increase the current density of the tape. This brings added difficulty manufacturing the conductor, as the substrate, among other components, are made thinner. With a better understanding of how to improve the conductor properties, REBCO coated conductor (CC) has become thinner. New technologies such as no-insulation (NI) magnets recommend a thinner copper (Cu) cross-sectional area for increased current densities and to allow construction of compact magnets. Other benefits of using REBCO CC include having a high critical current density ( $J_c$ ) at higher fields and “off the spool use,” without need for additional reaction or heat treatment before using the conductor.

### 1.4 Types of REBCO Coated Conductor

In this study, two manufacturers of REBCO CC, SuperPower and SuNAM, are used at the National High Magnetic Field Laboratory (NHMFL). Both manufacturers have a similar layer structure of how their REBCO CC is made, however, each uses a different vapor deposition process to grow the REBCO in the coated conductor. SuNAM uses a method called reactive co-evaporation by deposition & reaction (RCE-DR), while SuperPower uses a process called metalorganic chemical vapor deposition (MOCVD) to deposit the REBCO. One crucial difference between the two

manufacturers is their substrate. SuperPower uses cold-rolled Hastelloy<sup>®</sup> C-276, and SuNAM uses 310 stainless steel (SS), the significance of which will be discussed in more detail in later sections.

### 1.4.1 SuNAM REBCO CC

REBCO deposition by SuNAM utilizes the RCE-CDR process, which can be seen in Figure 1.1. The process starts with an electropolished 310 SS substrate that enters the ion beam assisted deposition (IBAD)-MgO process to promote proper texture alignment from the substrate to the REBCO layer. Then, the conductor is transferred to a conveyor-belt-like system where the rare earth metals, Ba, Ca and Cu, and various other elements including REBCO, are evaporated onto the substrate simultaneously in an oxidizing environment. Finally, silver is sputtered onto the REBCO and the conductor then is electroplated with copper. Figure 1.2 shows the layer structure of SuNAM REBCO CC with thicknesses of each layer. RCE-CDR has a rapid production rate for the REBCO layers by growing it in the liquid state in one continuous flow. The last step of the REBCO deposition, has the conductor go through both low and high PO<sub>2</sub> regions in a furnace for final reactions to occur. SuNAM’s manufacturing allows for extended lengths of tape at relatively fast production speeds, resulting in a cheaper REBCO CC.

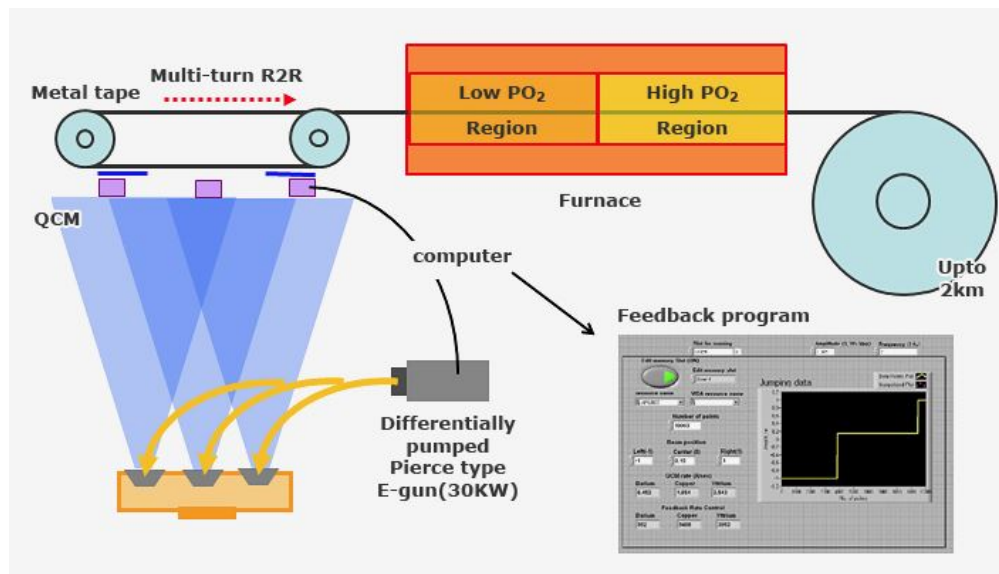


Figure 1.1: Visual representation of SuNAM CC manufacturing process using reactive co-evaporation by deposition & reaction [2].

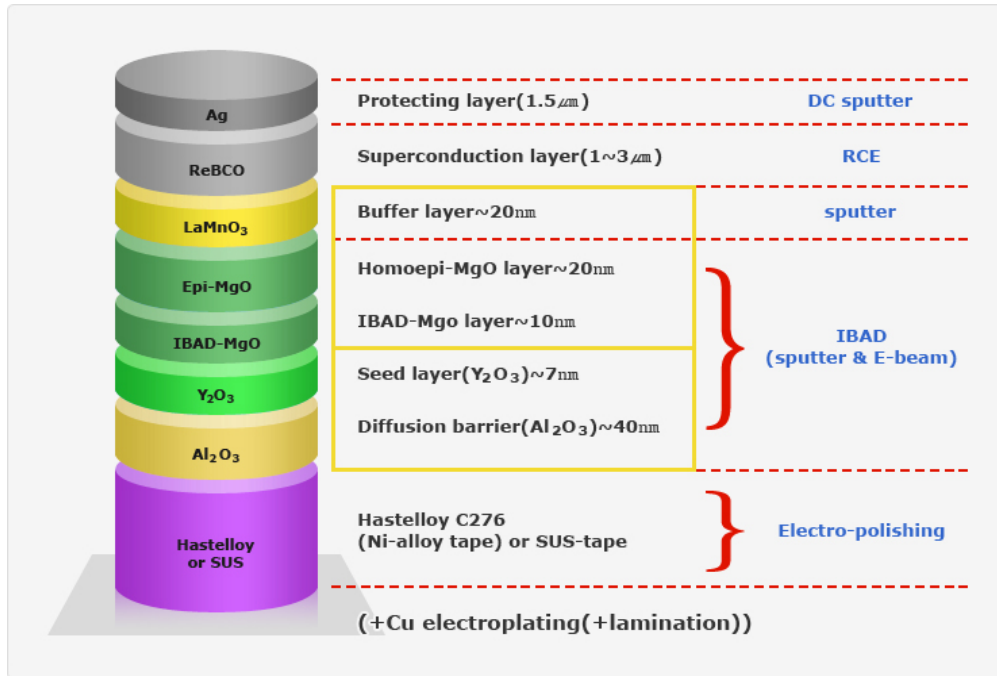


Figure 1.2: Diagram of SuNAM REBCO CC with individual layer thickness [2].

### 1.4.2 SuperPower REBCO CC

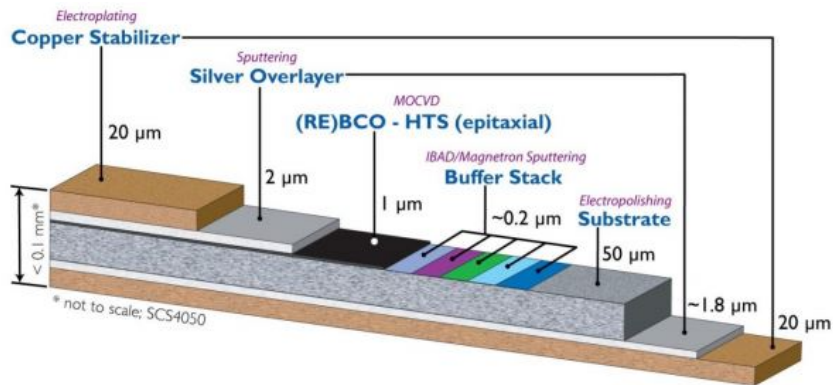


Figure 1.3: Diagram of SuperPower CC with individual layer thickness [3].

SuperPower, much like SuNAM, uses IBAD-MgO to deposit a strongly textured buffer layer onto the Hastelloy<sup>®</sup> substrate surface. However, SuperPower utilizes MOCVD to deposit the REBCO layer onto the buffer stack. The process begins with electropolished Hastelloy<sup>®</sup> to improve surface

smoothness from initial cold-working. A planarization layer of  $\text{Al}_2\text{O}_3$  coats the Hastelloy<sup>®</sup>, then the IBAD-MgO layer is grown on the substrate, heating the substrate to 700-800 °C [4]. Homo-epitaxial MgO growth occurs on the IBAD-MgO layer, an additional buffer layer of  $\text{CeO}_2$  or  $\text{Y}_2\text{O}_3$  is deposited, and then the MOCVD-REBCO layer is grown onto the buffer layers. Next, Ag is sputtered over the REBCO layer for protection. Lastly, a copper stabilizer is electroplated onto the conductor to stabilize it and to provide quench protection. Figure 1.3 shows the design of the SuperPower REBCO CC along with the thickness of each layer.

## 1.5 Introduction to Mechanics

This section provides background knowledge of the mechanics needed to understand the results of this study. A description of engineering stress, engineering strain, and the components that make up a stress-strain curve are given. An introduction to how uniaxial tension tests relate to stresses seen in solenoid magnets is also given.

### 1.5.1 Engineering Stress and Strain

Tension testing is often the most used mechanical test to benchmark the properties of materials. In tension, a material is subjected to a uniaxial force applied outward from the specimen as seen in Figure 1.4.

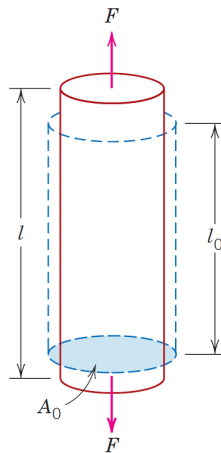


Figure 1.4: Schematic representation of uniaxial tension on a specimen with a change of length and diameter [5].

Engineering stress ( $\sigma$ ) is defined to be the applied force ( $F$ ) over the initial cross-sectional area ( $A_0$ ) of the specimen, seen in equation 1.1.

$$\sigma = \frac{F}{A_0} \quad (1.1)$$

Strain ( $\epsilon$ ) is defined to be the change of length ( $\Delta l$ ) over the original length ( $l_0$ ) as seen in equation 1.2.

$$\epsilon = \frac{l_i - l_0}{l_0} = \frac{\Delta l}{l_0} \quad (1.2)$$

When axial tension is applied to a specimen, a stress-strain curve can be plotted. This curve shows how much strain the specimen underwent at specific stresses.

In the linear elastic region of a stress-strain curve, the elastic modulus of a material can be determined by taking the slope seen in equation 1.3.

$$E = \frac{\sigma}{\epsilon} \quad (1.3)$$

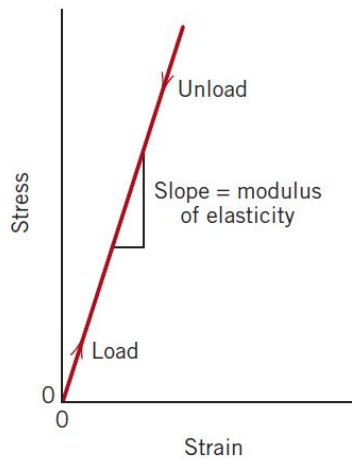


Figure 1.5: Linear elastic region of a stress-strain curve with the slope of the line defining elastic modulus  $E$ . [5].

Yielding of the material will occur once the stress within the specimen is high enough. Figure 1.6 shows a typical stress vs. strain curve demonstrating the onset of yielding.

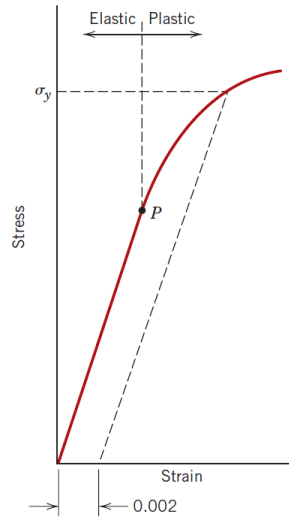


Figure 1.6: Stress vs. Strain curve with 0.2 yield strength offset, elastic and plastic regions, and approximately where the proportional limit is located [5].

Stress vs. strain curves can be divided into two main regions, the linear elastic region where deformation is reversible, and a plastic region where permanent damage is done. The red line shows what is called the 0.2 % offset yield strength ( $\sigma_{y,0.2}$ ). The yield strength of the material represents the point where permanent plastic deformation of the material occurs. This parameter becomes crucial in testing REBCO CC due to loss of superconducting performance from cracking the REBCO layer and yielding of the copper stabilizer.

### 1.5.2 Stress and Strain in Solenoid Magnets

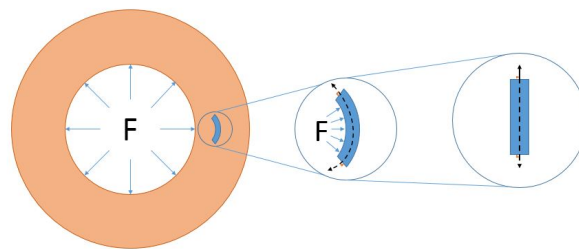


Figure 1.7: Representation of hoop stress in a solenoid magnet equating to uniaxial tension when the REBCO CC is wound along its neutral axis.

In solenoid magnet applications, superconducting wires or tapes are wound on a mandrel. This makes the conductor follow a circular path. When the magnet is energized, a Lorentz force will be produced causing stress to the conductor. The magnetic stress of unsupported turns due to the Lorentz force can be approximated by multiplying the field, current density, and radius of the magnet or coil ( $B \cdot J \cdot r$ ), while a uniaxial tension test on the conductor can predict how the Lorentz force will affect the conductor performance, as seen in Figure 1.7.

## 1.6 Defining Critical Current

Critical current is defined by a critical voltage or electric field relatable to the dissipation that will cause the magnet or coil to become normal. Insufficient cooling, over current, or damage to the conductor can all cause  $I_c$  degradation. For this study, only the critical current as a function of strain will be looked at. Two criterion conditions can be met to measure critical current, using 1 or  $0.1 \mu\text{V}/\text{cm}$ . The voltage and current can be plotted to determine the point where the conductor starts to dissipate and then the critical current can be found, seen in figure 1.8.

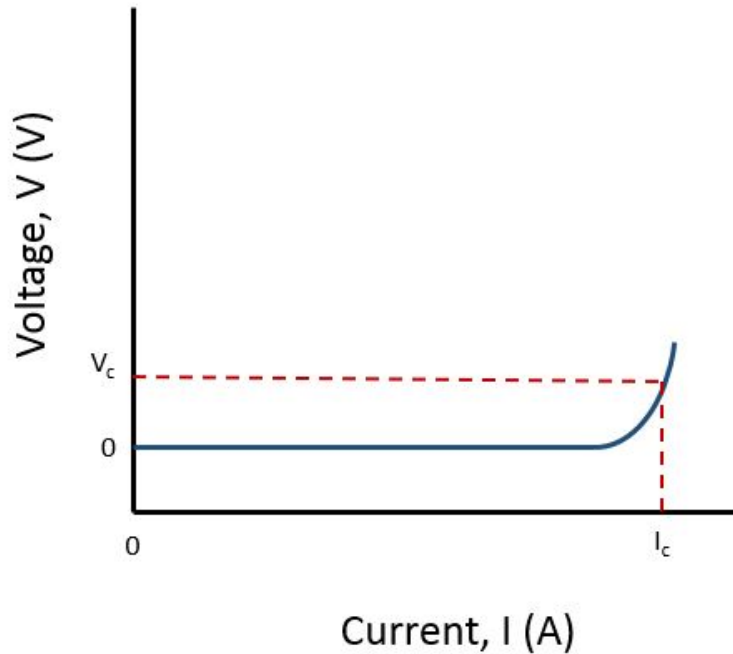


Figure 1.8: Voltage (V) vs. current (I) curve displaying the critical voltage and its corresponding critical current.

## 1.7 Literature Review

This section is to provide some details on how various other institutions perform or set guidelines to conduct the experiments done in this thesis. Other findings and distinguishing features of this work will also be presented in this section.

### 1.7.1 ASTM Standards & Guidelines

Three main standards are used in this study: ASTM E1450 [6], ASTM E111 [7], and ASTM E8 [8]. ASTM E8 sets rules on standard test methods for tension testing of metallic materials, ASTM E11 sets rules for determining elastic modulus and yield strength of materials, and lastly, ASTM E1450 sets the rules for testing materials in cryogenic environments.

### 1.7.2 SuperPower REBCO CC vs. Copper Thickness

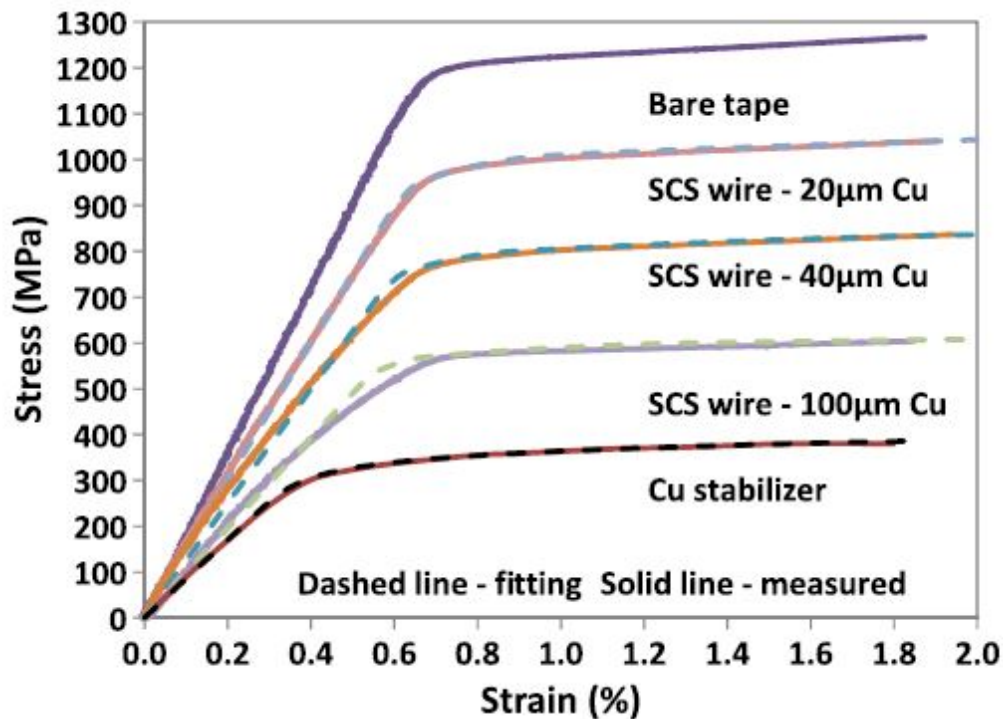


Figure 1.9: SuperPower REBCO CC stress vs. strain curves with each tape having 50 microns of Hastelloy<sup>®</sup> and varying copper thickness coated on each side of the conductor. Bare tape in this case indicates REBCO conductor without any copper stabilizer [9].

Mechanically speaking, the two primary contributors to the strength of REBCO CC are the substrate and the copper on the coated conductor. Zhang et al. [9] have done a systematic study on the effect of copper thickness on the strength of REBCO CC. Much like the work presented in this thesis, REBCO tapes were pulled in uniaxial tension, and the stress and strain were then measured. Figure 1.9 provides the results of stress vs. strain of REBCO CC with varying copper thickness. Each tape in the study had 50 microns of Hastelloy<sup>®</sup> with varying copper thickness. From the figure, it is quite evident that as the thickness of copper stabilizer increases, the effective Elastic modulus of the conductor is reduced.

Figure 1.10 shows the normalized critical current vs. strain of the same SuperPower REBCO CC tested in uniaxial tension done by Zhang et al. [9]. Mechanically, the conductor was heavily influenced by the copper thickness, however, regarding critical current vs. strain, the current carried within the conductor appeared to be independent of copper thickness.

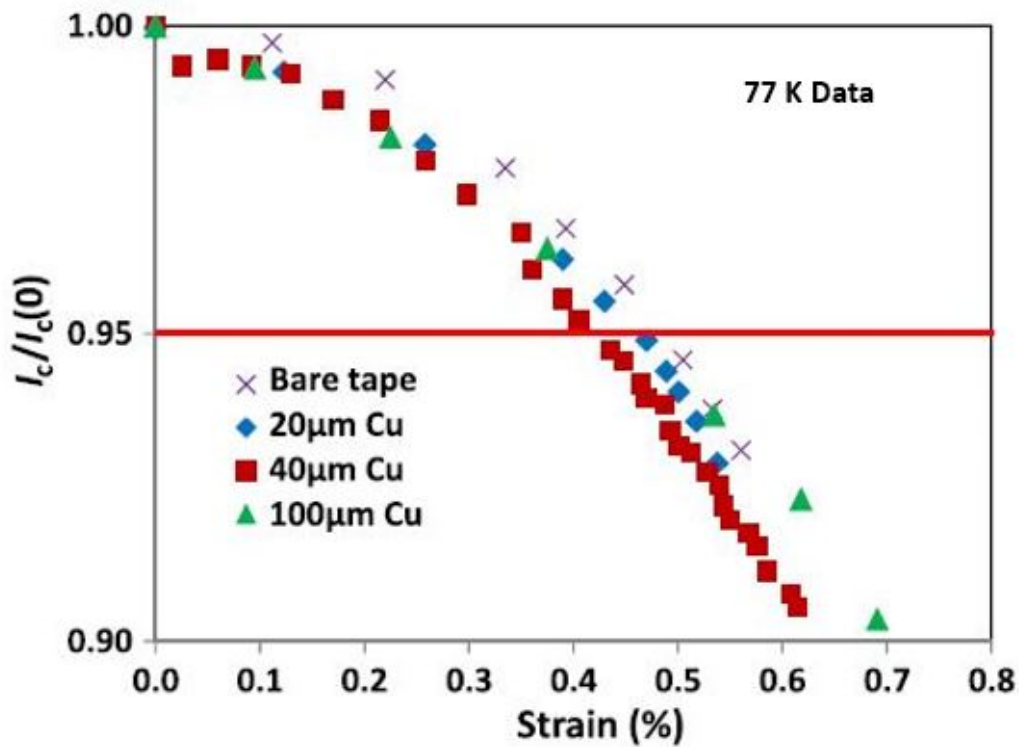


Figure 1.10: SuperPower REBCO CC critical vs. strain curves with each tape having 50 microns of Hastelloy<sup>®</sup> and varying copper thickness at 77 K [9].

# CHAPTER 2

## EXPERIMENTAL PROCEDURES

This chapter focuses on how the testing procedures were implemented, what instrumentation was used, how samples were prepared, and the expected uncertainties in the measurements. The two types of strain devices used in this thesis, how dimensions of the REBCO CC were recorded, and the two different mounting techniques for standard tensile and  $I_c$  vs. strain tests are presented.

### 2.1 Tensile Testing

A proper understanding of how each piece of equipment functions is key to ensuring that measurements are as accurate and precise as possible. A detailed description of each component required to perform tensile and  $I_c$  vs. strain tests is described in the next few sections.

#### 2.1.1 Tension Machine

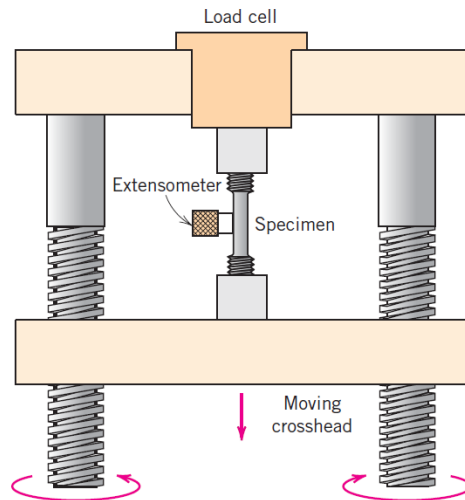


Figure 2.1: Schematic representation of a universal tension testing machine [5].

A standard tensile test is used to collect the mechanical properties of the REBCO CC. A universal tension testing machine, seen in Figure 2.1, is composed of a load cell, crosshead, and

a device to measure how much the specimen has deformed. The two types of devices used in this thesis were a strain gage and a two-inch extensometer. The crosshead can move upward or downward to apply tensile or compressive uniaxial force to the specimen causing deformation. The extension recorded by the strain devices can then be converted into strain. A load cell measures how much force is being applied to the specimen.

### 2.1.2 Strain Gages

A strain gage is a type of sensor that is bonded directly to the specimen so as to detect the material's deformation. When the material is experiencing a force, the strain gage's resistance wires, seen in Figure 2.3, will deform with the material creating a change of resistance ( $\Delta R$ ). This change in resistance is due to elongation or compression of the material, thereby changing its cross-sectional area and length as seen in Figure 2.2. The Karma alloy strain gage used is a nickel chromium alloy [10] that has a known resistivity ( $\rho$ ) which is used in Equation 2.1 to calculate the resistance of the material.

$$R = \rho \frac{L}{A} \quad (2.1)$$

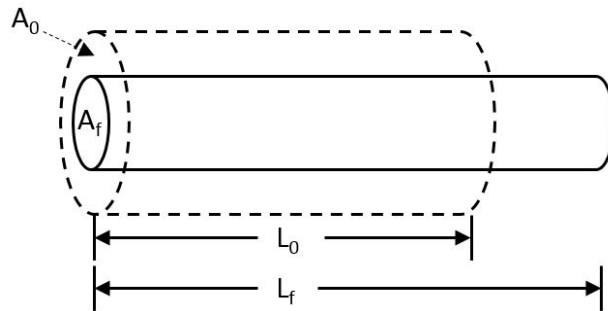


Figure 2.2: Graphical representative of a uniformed wire changing shape uniformly, altering its internal resistance.

The amount of voltage created by deformation is controlled by the sensitivity of the strain gage known as the gage factor (GF). By using Equation 2.2 and knowing the GF, the change of length ( $\Delta L$ ) can be found. A karma alloy strain gage with a GF of +2.06 and 350  $\Omega$  resistance (R) was used for this study.

$$\frac{\Delta L}{L} = \frac{1}{GF} \frac{\Delta R}{R} \quad (2.2)$$

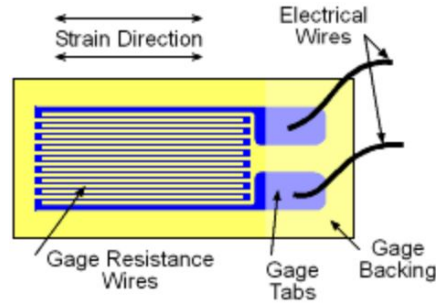


Figure 2.3: Strain gage schematic showing the direction along which the gage can measure strain, and the resistance wires whose change in resistance when deformed determines the strain value [11].

Mounting a strain gage requires a two-part glue mixture to be applied to the sample and then cured in an oven at 60°C for two to three hours. Alignment of the strain gage is crucial as misalignment will cause inaccurate strain measurements. A tilted strain gage will not measure uniaxial tension, giving false results. In a later chapter, using a strain gage on REBCO CC yields unfavorable results as this will locally reinforce the area under the strain gage causing what is called the *strain gage reinforcement effect*.

### 2.1.3 Extensometer

The extensometer used in this study is a reusable clip-on device that detects the change in length of the specimen. Four strain gages in a Wheatstone bridge configuration are attached to the thin bending arm of the extensometer. As the material elongates or compresses, the strain gages attached to the extensometer average the displacement the specimen is experiencing. With a known gage length (GL), and a measure of how much the extensometer extended, the amount of strain the specimen experiences can be calculated using Equation 2.3. Figure 2.4 shows the two-inch clip-on Shepic extensometer used in this study. Knife edges lightly clip onto the specimen without damaging the sample but with enough spring force to prevent slip during the experiment.

$$\epsilon = \frac{Extension}{GL} \quad (2.3)$$

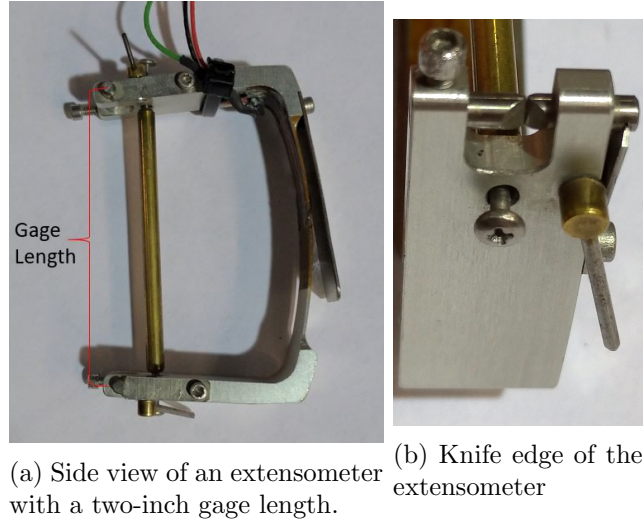


Figure 2.4: Two-inch Shepic extensometer with a side view (a) and knife edge shape (b).

## 2.2 Sample Preparation

SuNAM REBCO CC are nominally 4 mm wide and 120  $\mu\text{m}$  thick, making it easy to bend or kink. This section will go over the procedure to mount and measure the dimensions of the conductor. Dimensional width and thickness variation becomes a critical factor as the conductor is not uniform nor rectangular. Specialized grips are made to hold the thin conductor for tensile tests and to offer efficient current transfer for  $I_c$  vs strain tests.

### 2.2.1 Dimensions of REBCO CC

Knowledge of the cross-sectional area of REBCO CC is essential for understanding magnet performance and is also crucial for the assessment of the electromechanical properties. The average area of a test specimen is important as it is used to obtain engineering stress values.

In this study, 4 mm wide conductors were used to perform a series of experiments. The 4 mm conductor width was initially a 12 mm wide tape until all components of the conductor is vapor deposited on the metal substrate. The tape is then slit into three separate 4 mm wide tapes, with each tape electroplated with copper. Figure 2.5 provides a cross-sectional view of SuNAM REBCO with a nominal width of 4 mm and a nominal thickness of 120 microns. The cross-sectional view of the conductor shows the non-uniformity of the electroplated copper surface, especially near the

slit edge of the tape. Due to the imperfect surface of the copper, artificial high and low spots could be measured. Since engineering stress is a function of the cross-sectional area, artificial high and low spots on the conductor surface can misrepresent the actual cross-sectional area. These imperfections on the surface of the conductor need to be taken into account for proper analysis.



Figure 2.5: Cross-sectional view of SuNAM REBCO CC with 100 microns of 310 SS and 7.5 microns of copper on each side.

To combat the issue of properly recording the dimensions of REBCO CC, nine points of thickness and three points of width are taken within the gage length of the extensometer, as seen in Figure 2.6.

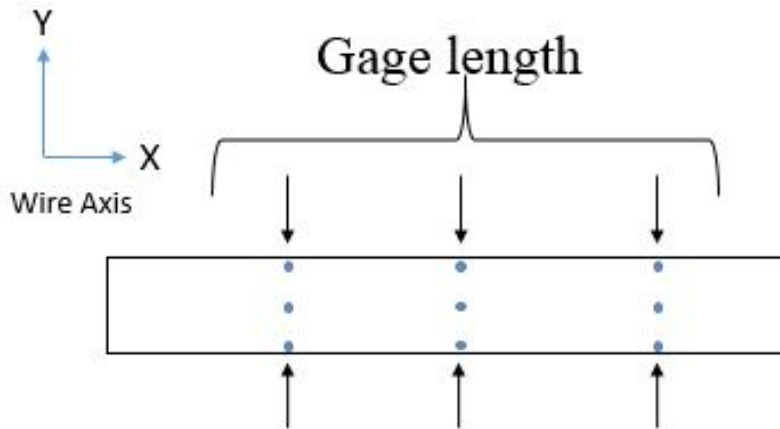


Figure 2.6: Schematic diagram of how sample dimensions are taken where tape length is in the x-direction and the width is in the y-direction. Dots represent points where the thickness is taken, while arrows show where the points the width is taken.

The thickness is measured by a micrometer with a resolution of  $\pm 1 \mu\text{m}$ , while the width is measured by an optical microscope with a resolution of  $\pm 1 \mu\text{m}$ . Thickness and width are then averaged to obtain an average area for each specimen.

Table 2.1: Variation of conductor thickness and width of SuNAM CC

Batch No.	Spool Number	Tensile Spec No	Thickness (outside-inside-outside)			Width mm	Avg Area $mm^2$
			mm	mm	mm		
160819	-04	1	0.119	0.117	0.118	4.03	0.482
			0.119	0.119	0.119	4.02	
			0.123	0.121	0.122	4.03	
160804	-04	2	0.122	0.123	0.123	3.97	0.477
			0.120	0.121	0.120	3.98	
			0.118	0.117	0.117	3.97	
160729	-02	2	0.119	0.118	0.119	4.04	0.486
			0.120	0.119	0.120	4.05	
			0.122	0.121	0.122	4.05	

Table 2.1 shows the measured dimensions of thickness, width, and calculated cross-sectional area of three SuNAM REBCO CC samples. Variation of thickness can be easily seen in the measurements, providing proof of non-uniformity in the electroplating process for the copper stabilizer. The SuNAM tapes used in this study have a nominal thickness and width of  $120 \mu\text{m}$  and  $4 \text{ mm}$ , respectively, as reported by SuNAM. A total of 32 REBCO CC samples were measured 300 times collectively, resulting in an average of  $120 \mu\text{m}$  and a standard deviation of  $1.57 \mu\text{m}$ . Appendix A.1 reports all SuNAM REBCO CC dimensions used for testing.

### 2.2.2 Uncertainty Analysis

The dimensions of REBCO CC can be difficult to measure when the electroplating process creates a non-uniform cross-sectional area along its width and length. This non-uniformity could cause an error when measuring the area, especially in thickness measurements of tapes. A brief analysis shows the effect of varying cross-sectional area from the thickness measurements. The micrometer can measure the thickness of the conductor to  $\pm 0.83 \%$ , the optical microscope used to measure the width can measure to  $\pm 0.025 \%$ , and the 1000 N load cell can measure to  $\pm 0.1 \%$ . Since stress is a function of area, the uncertainties can propagate to produce a significant final error.

$$(120\text{mm} \pm 0.83\%) * (4\text{mm} \pm 0.025\%) = 0.480\text{mm}^2 \pm 0.86\% = \text{area}$$

$$\frac{1000\text{N} \pm 0.1\%}{0.480\text{mm}^2 \pm 0.86\%} = 2083\text{MPa} \pm 0.96\% = \text{stress}(\sigma)$$

If the thickness is measured with a resolution of  $\pm 10 \mu\text{m}$ .

$$(120\text{mm} \pm 8.33\%) * (4\text{mm} \pm 0.025\%) = 0.480\text{mm}^2 \pm 0.836\% = \text{area}$$

$$\frac{1000\text{N} \pm 0.1\%}{0.480\text{mm}^2 \pm 0.836\%} = 2083\text{MPa} \pm 8.46\% = \text{stress}(\sigma)$$

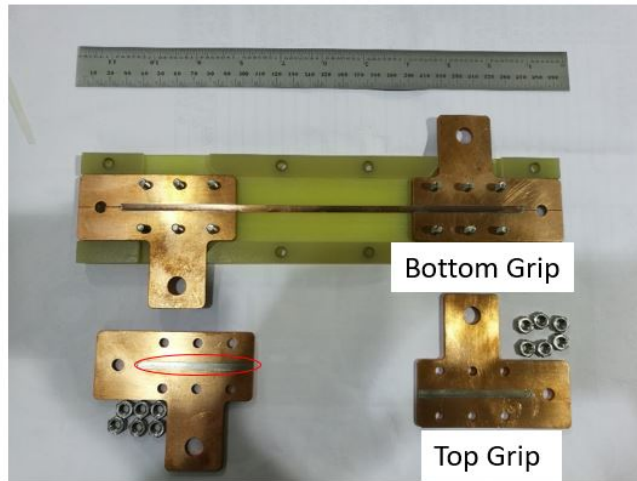
The resulting uncertainty increase from 0.96 % to 8.46 % in the final stress result. To reiterate, the resolution of the thickness measurements are within  $\pm 1 \mu\text{m}$ , resulting in a final error of 0.96 %. This example demonstrate the importance of refined techniques and procedures when measuring the dimensions of REBCO CC, and the positive effects of taking more measurements for the cross-sectional area and following ASTM standards.

### 2.2.3 Mounting REBCO CC

Two types of mounting grips were used depending on the tensile or critical current vs strain test being performed. Figure 2.7 (a) shows one side of a tensile testing grip that is lined with sandpaper to mitigate slipping during the test, (b) shows the grips for the  $I_c$  vs. strain test that were embedded with tinned REBCO CC in both the bottom and top grip so as to be able to carry current from grips to the sample.



(a) Tension testing grip lined with sandpaper.



(b)  $I_c$ -strain grip with tinned REBCO CC (red circle) in bottom and top grips.

Figure 2.7: Mounting grip for (a) tensile test and (b)  $I_c$  vs. strain test.

## 2.3 Tensile Test Procedure

The REBCO CC test sample is initially attached to the top grip only and then placed into the tension machine. The load cell is then “zeroed” to offset the weight of the pull rods and top grip, before it applies any force onto the conductor. After the load cell is zeroed, the bottom grip is attached to the sample. Scribe marks located on both grips help align the specimen. An initial load of 25 N is loaded onto the sample to keep it aligned, but not enough to damage the REBCO CC. The extensometer is then placed at the center of the sample. Figure 2.8 shows the final mounting. Testing can begin after cooling the fixture to 77 K in a bath of liquid nitrogen and zeroing the extensometer once thermal contraction reaches a steady state. The cross-head moves at a rate of 0.5 mm/min until the 50 mm gage length extensometer extends 0.3 mm  $\sim$  0.6 % strain and is then reloaded until the specimen reaches approximately 1 % strain.

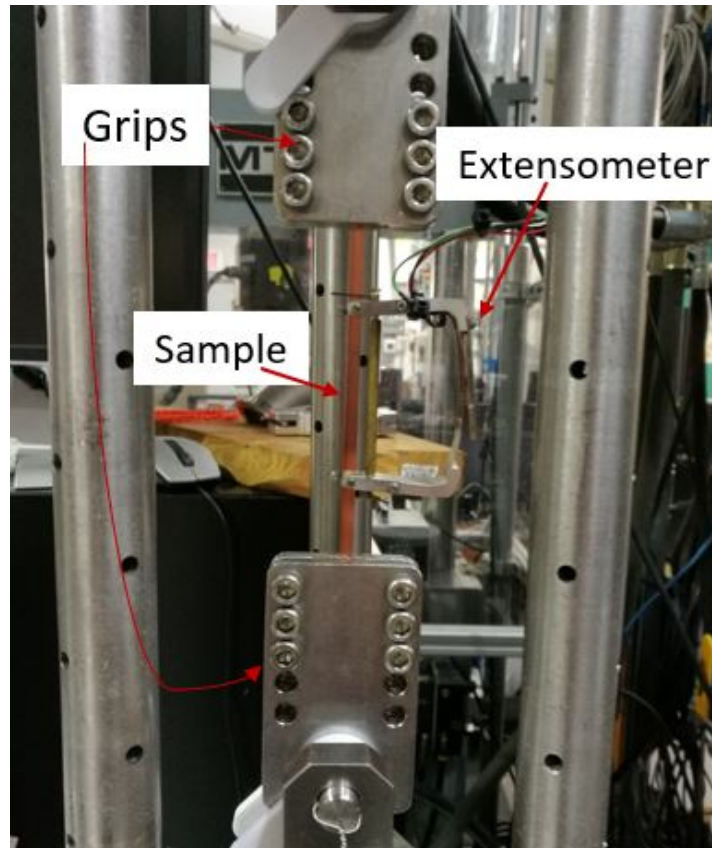


Figure 2.8: Final mounting of REBCO CC for tensile tests.

## 2.4 Critical Current vs Strain Test Procedure

Critical current vs. strain tests have a testing procedure similar to a tensile test. Before the sample is mounted into the copper grips, the surface of the specimen and grips are cleaned with acidic, deoxidizing agent, such as APS-100, to improve contact conductance. The weight of the top grip, current leads, and G-10 guide is zeroed from the load cell. The bottom grips are then attached, and an initial load of 25 N is loaded onto the specimen. Current leads connect in four locations, as seen in Figure 2.9, to help current transfer into the sample. A notch in the G-10 guide allows for the use of a 25.4 mm extensometer if needed. Voltage tabs are placed on the center of the conductor and near the grip to monitor the voltage during current ramping and to find the critical current. The sample is then cooled to 77 K in a bath of liquid nitrogen, and without any strain, an initial critical current is measured. Strain in the sample is increased incrementally in steps of 0.025 % strain, and  $I_c$  is again measured and recorded manually. The sample is then unloaded to the strain-free condition to detect any  $I_c$  degradation after straining the sample. This process continues until the sample can no longer carry current.

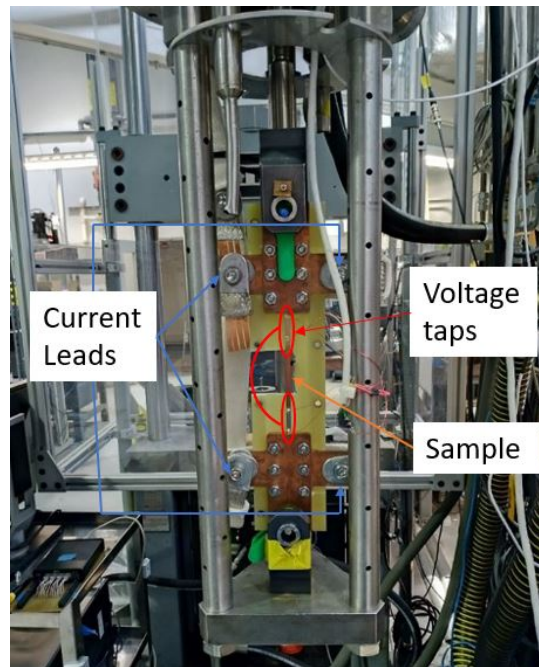


Figure 2.9: Critical current vs strain mount inside a tension machine. Red circles indicate voltage taps placement, sample location, and current leads locations from the power supply.

# CHAPTER 3

## RESULTS

This chapter shows the initial results of three different types of tests performed on REBCO CC. A systematic study of 18 tensile tests and ten critical current vs. strain tests of SuNAM REBCO CC will be reported in this chapter. Three different heat treatments at 700, 750, and 800 °C were performed on on Hastelloy<sup>®</sup> and 310 SS substrates were done in order to assess the effects of small variations in the deposition process. The final section will present the impact of strain on critical current for SuNAM REBCO CC.

### 3.1 Stress-Strain Dependence on Different Batches SuNAM REBCO CC

#### 3.1.1 Batch 1 Fabricated July 29, 2016

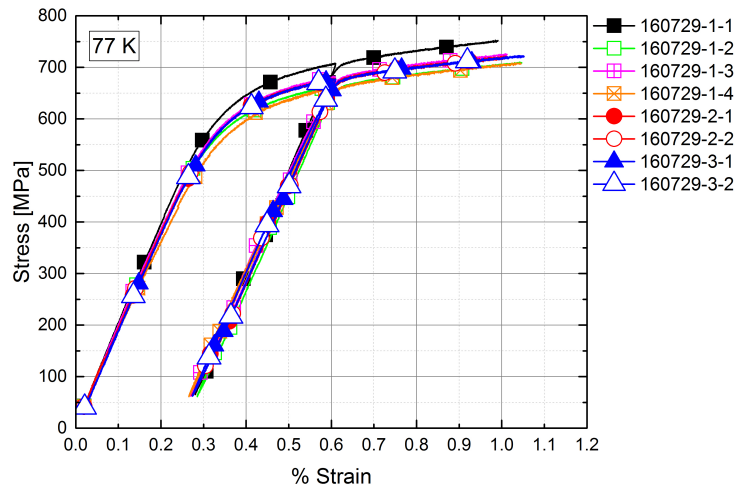


Figure 3.1: Stress vs. strain of SuNAM REBCO CC manufactured on July 29<sup>th</sup>, 2016 (160729). Symbols do not represent the number of data points taken. Like symbols (i.e., squares, circles, and triangles) indicate different acquired taken from the same spool. Legend reads as follows, 160729-X-X: manufactured date-spool number-sample number.

Figure 3.1 shows the stress vs. strain dependence of eight SuNAM REBCO CC samples made on July 29<sup>th</sup>, 2016. Samples are labeled in order of manufactured date-pool number-sample number and with symbols to show the general trend of the results (symbols do not represent the number of data points). All SuNAM REBCO CC samples had a total nominal thickness of 120  $\mu\text{m}$ , with 100  $\mu\text{m}$  310 SS substrate, 15  $\mu\text{m}$  of copper, and 1- 1.5  $\mu\text{m}$  of REBCO. The elastic modulus (E) ranged from 190-191 GPa, with an average of 190 GPa. 0.2 % yield strength ( $\sigma_{0.2}$ ) ranged from 652-697 MPa, with an average of 667 MPa. Sample 160729-1-1 showed a stress-strain curve higher than the other samples tested, even with samples taken from the same pool (160729-1-2,160729-1-3, and 160729-1-4).

### 3.1.2 Batch 2 Fabricated August 4, 2016

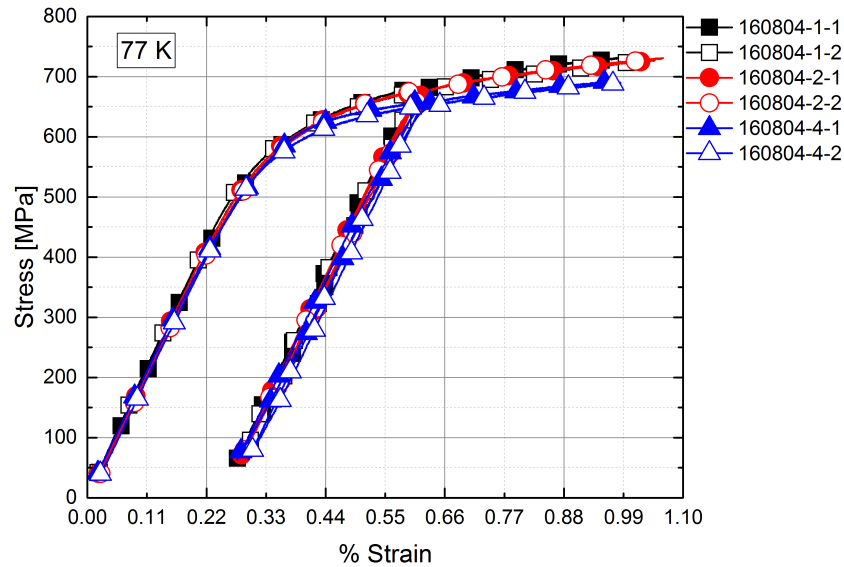


Figure 3.2: Stress vs. strain of SuNAM REBCO CC manufactured on August 4<sup>th</sup>, 2016 (160804). Symbols do not represent the number of data points taken. Like symbols (i.e., squares, circles, and triangles) indicate different samples taken from the same pool. Legend reads as follows, 160804-X-X: manufactured date-pool number-sample number.

Slight differences in pool stress-strain behavior can be seen in Figure 3.2. Six SuNAM REBCO CC samples from production date August 4<sup>th</sup>, 2016 (160804) were tested. The linear elastic regions

of the samples match well until yielding starts to occur.  $E$  ranged from 187-193 GPa with  $\sigma_{0.2}$  ranging from 638-669 MPa. The average of the results equates to an  $E$  of 190 GPa and  $\sigma_{0.2}$  of 657 MPa. Referring back to Figure 3.1, a similar phenomenon occurred in one of the samples from spool 4 which was different from the rest of the batches made on the same day.

### 3.1.3 Batch 3 Fabricated on August 19,2016

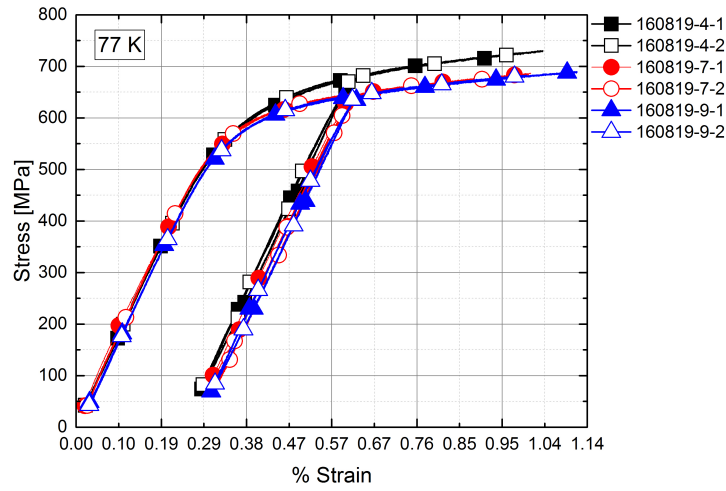


Figure 3.3: Stress vs. strain of SuNAM REBCO CC manufactured on August 19<sup>th</sup>, 2016 (160819). Symbols do not represent the number of data points taken. Like symbols (i.e., squares, circles, and triangles) indicate different samples taken from the same spool. Legend reads as follows, 160819-X-X: manufactured date-spool number-sample number.

Figure 3.3 represents six stress vs. strain curves SuNAM REBCO CC manufactured on August 19<sup>th</sup>, 2016 (160819). What is intriguing about these results is that the samples fall into two samples, 160819-4-1 and 160819-4-2, showing higher strength after passing the  $\sigma_{y,0.2}$  than the other four. Much like the previous results from batches 1 and 2,  $E$  of batch 3 matched well until the onset of yielding occurred.  $E$  ranged from 185-193 GPa with an average of 188 GPa and  $\sigma_{0.2}$  ranging from 628-667 MPa with an average of 643 MPa. All three batches of SuNAM REBCO CC had similar elastic modulus but differences of plastic properties of  $\sigma_{y,0.2}$  summarized in Table 3.1. In discussion of this variation ( $\sigma_{y,0.2}$ :batch 1=667 MPa, batch 2=657 MPa, and batch 3=643 MPa), we wondered

whether the 310 SS substrate was being partially recovered during the REBCO deposition process. This prompted a study of the effect of annealing in the 700-800 °C range for SuNAM substrate.

Table 3.1: Table of summarized results for the range and average  $\sigma_{0.2}$

Batch #	Average $\sigma_{0.2}$ MPa	$\sigma_{0.2}$ MPa
1	667	652-697
2	657	638-669
3	643	628-667

### 3.2 Simulated Heat Treatment Effects of the REBCO Deposition Process on Hastelloy<sup>®</sup> and 310 SS Substrates

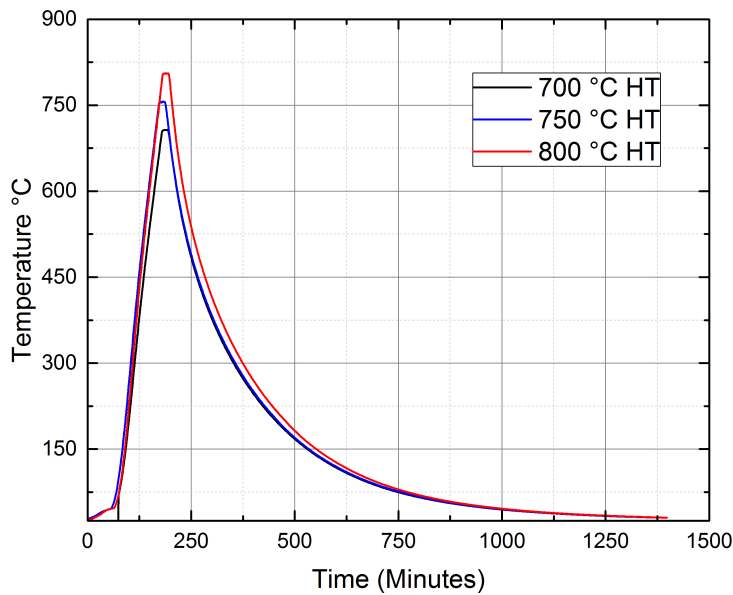


Figure 3.4: Temperature profiles of the simulated REBCO deposition heat treatments at 700, 750, and 800 °C.

Four substrate conditions were tested to study the effect of heat treatment during the vapor deposition process. As received, and 15 minute anneals at 700, 750, and 800 °C samples showed

how sensitive the 50 and 30  $\mu\text{m}$  Hastelloy<sup>®</sup> C-276 and 100  $\mu\text{m}$  310 stainless steel substrates were to temperature in the REBCO deposition range. Figure 3.4 shows the temperature profiles for the heat treatment. Ramping to temperature took approximately three hours and the samples were then held at temperature for 15 minutes. After the heat treatments, the samples were air cooled. All heat treatments were done in an argon environment and tensile tested at room temperature.

### 3.2.1 As Received Condition

Figure 3.5 shows the tensile tests for the substrates in the as received condition. The average elastic modulus of the Hastelloy<sup>®</sup> and 310 stainless steel are 181 and 174 GPa, respectively. Yield strength ( $\sigma_{0.2}$ ) for the 310 stainless steel is 1237 MPa, while the Hastelloy<sup>®</sup> is 1464 MPa. 50 and 30  $\mu\text{m}$  Hastelloy<sup>®</sup> substrate matched well with each other. However, due to a possible misalignment in mounting the samples, the 310 stainless steel samples have a discrepancy in the E and  $\sigma_{0.2}$ . However, both substrates demonstrated high strength mechanical properties.

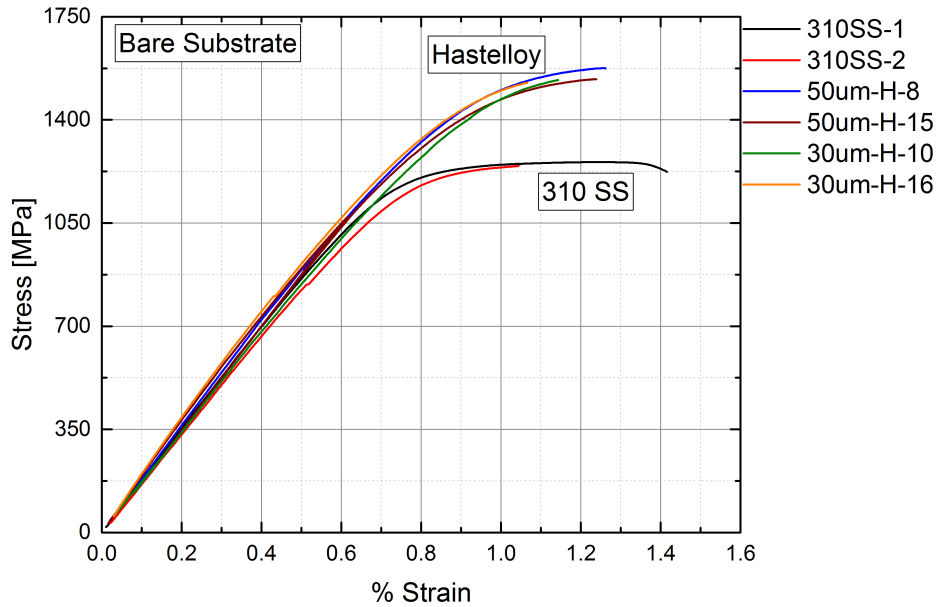


Figure 3.5: Stress-strain dependence on as received Hastelloy<sup>®</sup> and 310 stainless steel, where 310SS-1 represents the type and sample number of the steel substrate tested, and H represents Hastelloy<sup>®</sup> with -8 indicating sample number. Test was performed at room temperature

### 3.2.2 Effects of 700 °C Heat Treatment

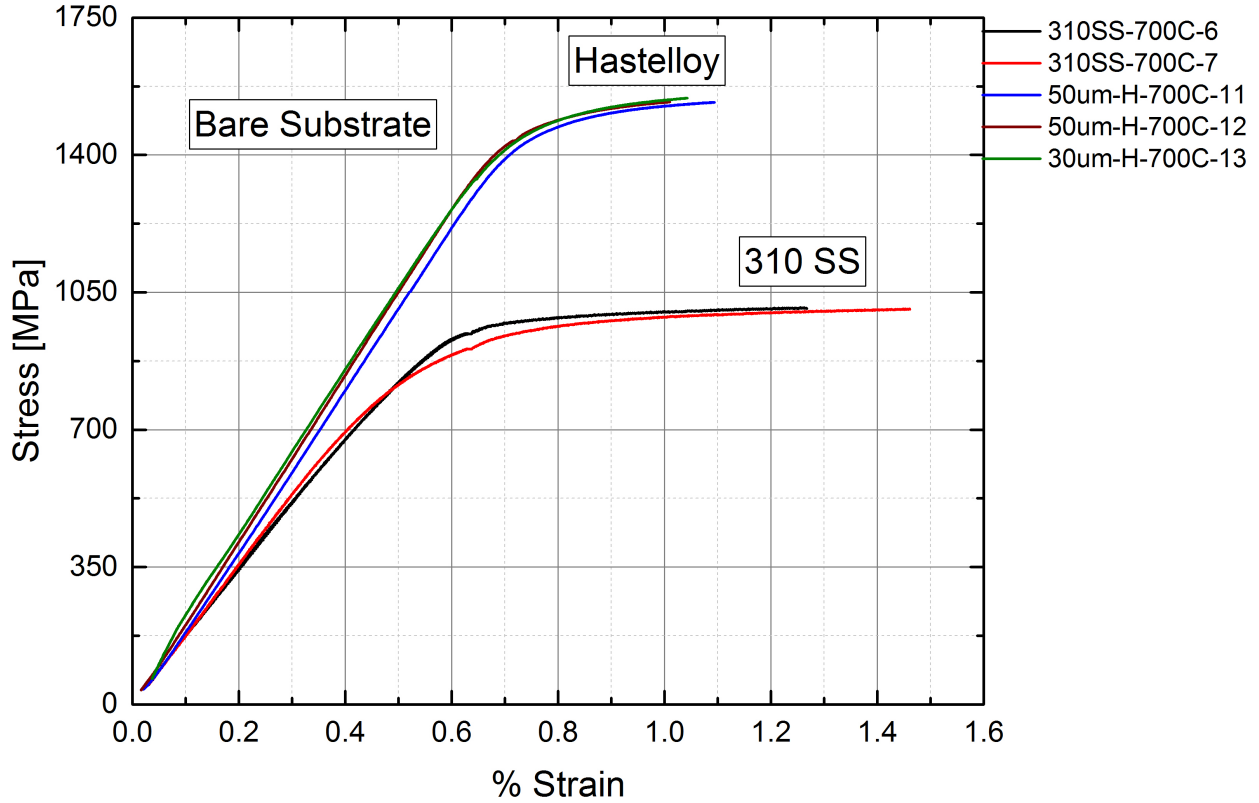


Figure 3.6: Effect of 700 °C simulated vapor deposition heat treatment Hastelloy and 310 stainless steel bare substrate.

Simulation of the REBCO deposition process with a 700 °C heat treatment yielded an quite unexpected result. The substrates were held at temperature for 15 minutes, the initial hypothesis being that nothing should happen to the strength of the materials, because Hastelloy<sup>®</sup> and 310 stainless steel both have annealing temperatures around 1100 °C. What is seen in Figure 3.6 is that the strength of both substrates changed. Hastelloy<sup>®</sup> improved its  $\sigma_{0.2}$  yield strength from 1464 MPa to 1524 MPa, while the 310 stainless steel decreased its  $\sigma_{0.2}$  yield strength substantially from 1237 MPa to 965 MPa.

### 3.2.3 Effects of 750 °C Heat Treatment

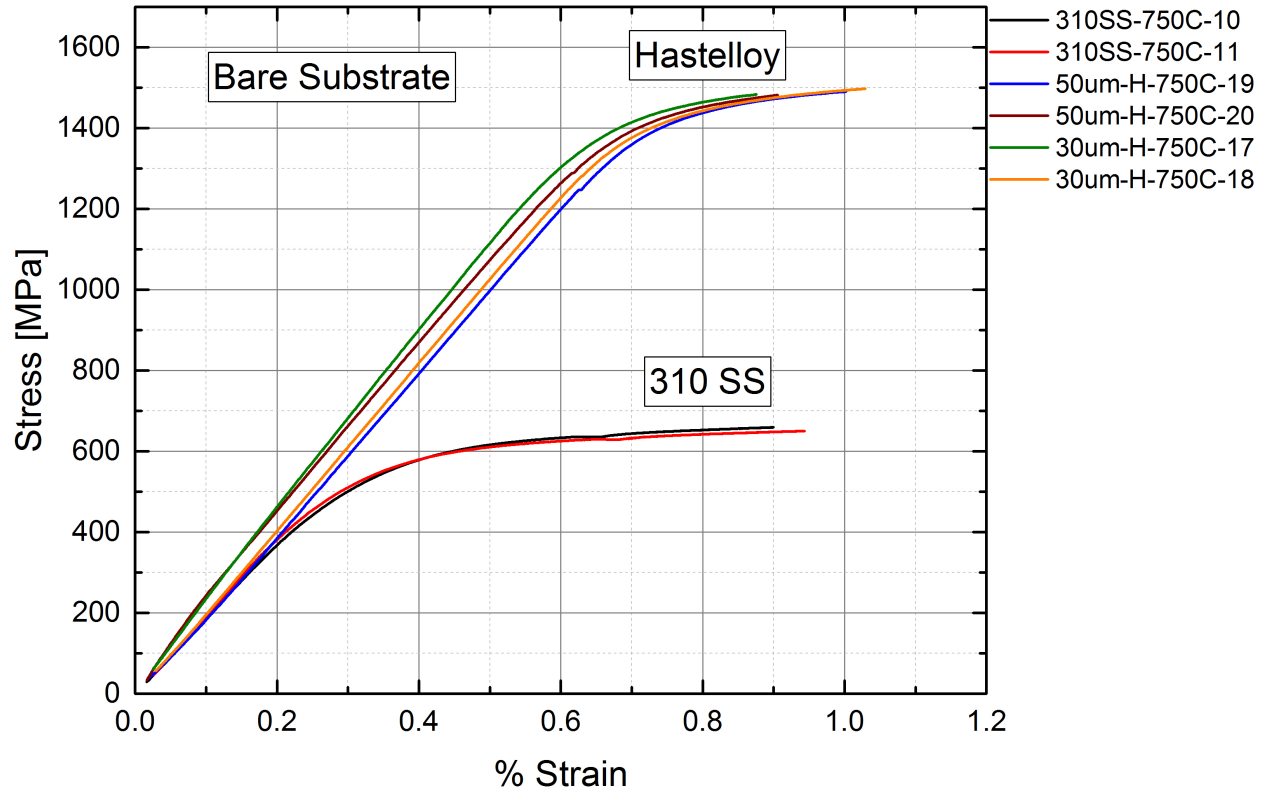


Figure 3.7: Effect of 750 °C simulated REBCO deposition heat treatment on bare Hastelloy and 310 stainless steel substrates.

A heat treatment of 750 °C causes little change in the Hastelloy<sup>®</sup> properties when compared to the 700 °C heat treatment. However, a closer look at Figure 3.7 shows a range of elastic moduli of the Hastelloy<sup>®</sup> ranging from 205-217 GPa, with the 310 stainless steel substrate ranging from 185-190 GPa. The 310 stainless steel substrate does get much weaker, lowering its  $\sigma_{0.2}$  yield strength from 1237 MPa to 619 MPa. Hastelloy<sup>®</sup>  $\sigma_{0.2}$  yield strength stayed relatively the same at 1477 MPa when compared to the as received condition at 1464 MPa.

### 3.2.4 Effects of 800 °C Heat Treatment

The yield strength of the 310 stainless steel substrate was lowered even further from 1237 MPa to 710 MPa after the simulated heat treatment at 800 °C, when compared to the as received condition value of 1237 MPa. Similarly, Hastelloy<sup>®</sup> also lowered its  $\sigma_{0.2}$  strength by about 240 MPa, compared to the initial substrate condition of 1464 MPa. Mechanical variability can be seen in Figure 3.8, in particular, with respect to the elastic modulus of the material. One possible reason for an almost flat yielding point is due to the precipitation hardening of the Hastelloy near its optimum precipitation temperature of 871 °C forming titanium precipitates [12].

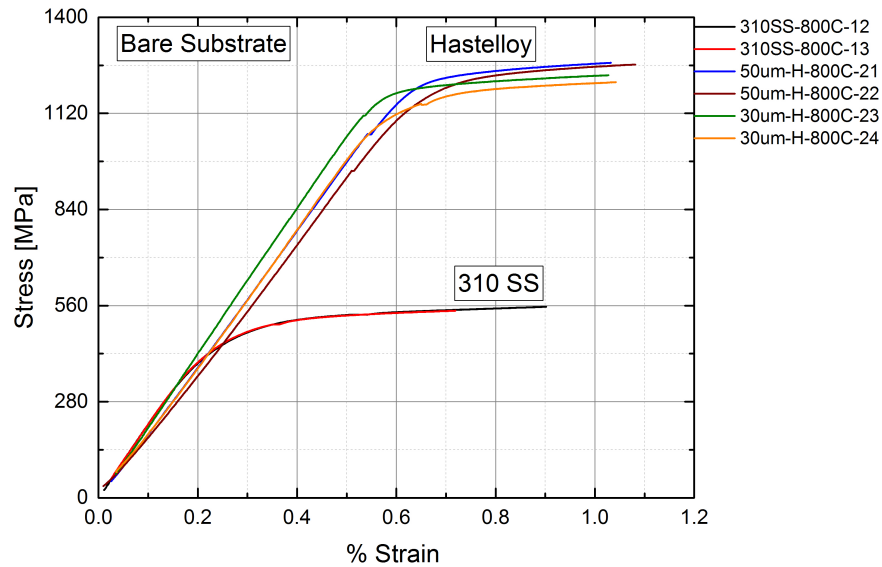


Figure 3.8: Effect of 800 °C simulated REBCO deposition heat treatment on bare Hastelloy and 310 stainless steel substrates.

### 3.3 $I_c$ -Strain Dependence of Different Batches on SuNAM REBCO CC

Mechanically, the strength of the SuNAM CC is much less than the strength of SuperPower CC. This is primarily due to SuperPower using Hastelloy<sup>®</sup> C-276 as their primary support, as opposed to SuNAM using 310 stainless steel. In this section, a total of 10 samples were tested on

the three different SuNAM batches. All results were normalized using Equation 3.1, where  $I_c(\epsilon)$  is the critical current while being strained,  $I_c(0)$  is the critical current under no load, and  $I'_c$  is the normalized critical current.

$$I'_c = \frac{I_c(\epsilon)}{I_c(0)} \quad (3.1)$$

### 3.3.1 Batch 1 Fabricated July 29, 2016

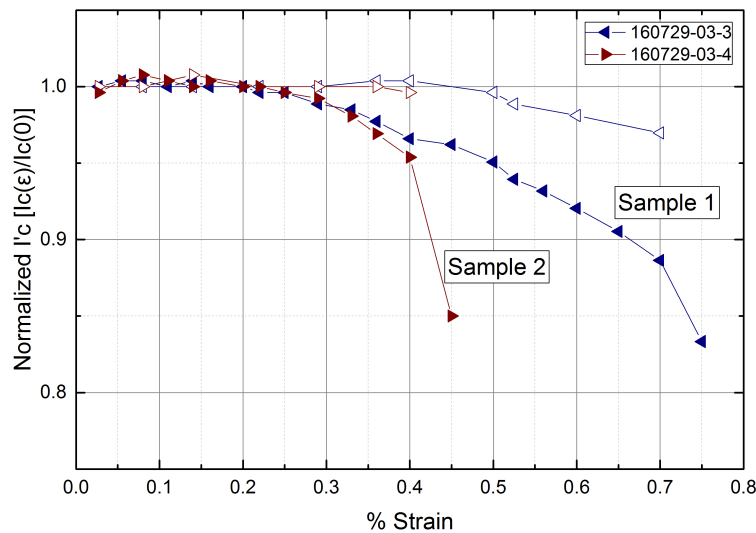


Figure 3.9: Normalized critical current vs. strain of SuNAM CC batch 1 (160729). Closed symbols represent the critical current while the sample was under load and open symbols show the critical current at the no-load condition after the strain was applied at 77 K.

Two samples of SuNAM CC batch 1, were tested at 77 K to measure the strain effects on current carrying capabilities. Each sample started with an initial load of 25 N or about 0.027 % strain, where the first critical current point was taken. After the initial critical current measurement was taken, the strain was increased incrementally and then returned to the initial condition to retest the critical current. At 0.3 % strain, the normalized  $I_c$  started to drop off considerably for both samples. When comparing Sample 2 to Sample 1, Sample 2 had a steeper drop in performance after 0.4 % strain. When the strain was removed, the normalized critical current returned to back

to its initial condition, as if no damage had occurred to the conductor. We also can define critical strain ( $\epsilon_{c,0.95}$ ) and irreversible strain ( $\epsilon_{irr,0.99}$ ) to represent the strain limits where the normalized  $I_c$  drops to 99 and 95 %, respectively, of the initial normalized current. Critical strain results are obtained from REBCO CC while under load and, irreversible strain is obtained from the unload data. The  $\epsilon_{c,0.95}$  is 0.4 and 0.5 % for both samples, and  $\epsilon_{irr,0.99}$  is 0.52 %.

### 3.3.2 Batch 2 Fabricated August 4, 2016

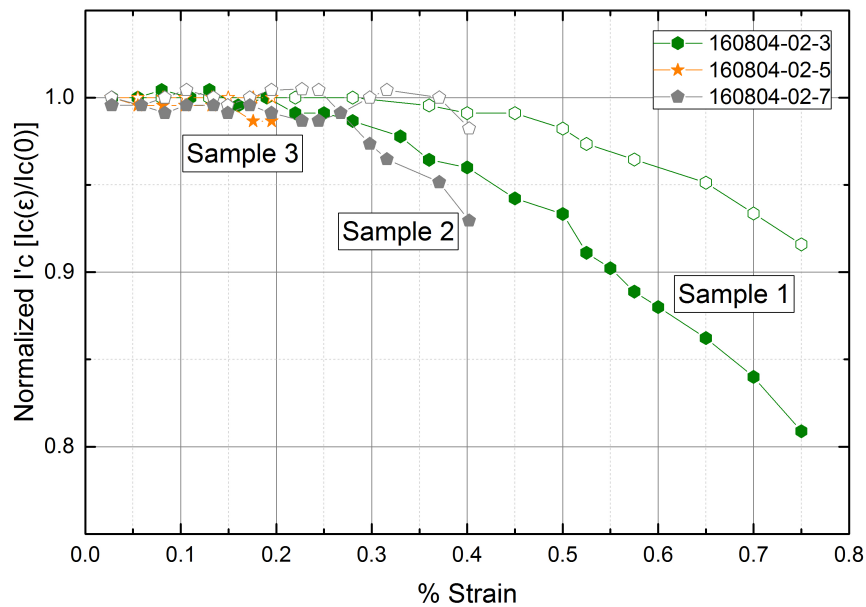


Figure 3.10: Normalized critical current vs. strain of SuNAM CC batch 2. Closed symbols represent the critical current while the sample is under load and open symbols show the critical current at the no-load condition after the strain was applied at 77 K. Strain from samples 160804-02-5 and 160804-02-7 strain was measured using a one-inch clip-on extensometer.

Three samples from batch two were also subjected to the same critical current vs. strain measurements as batch 1. Samples 160804-02-5 (yellow star) and 160804-02-7 (gray pentagon) had strain measured using a one-inch clip-on extensometer. The extensometer was isolated from the samples so that no current could be transferred through it, which would produce misleading results, batch 1, however did not have the extensometer attached. Sample 160804-02-5 did not offer as much

data due to a burn out near the grips. In this batch, the specimens started to lose current-carrying capacity when the strain reached about 0.22 % and continued to drop, where batch one started to drop after 0.27 % strain. Test samples that ended abruptly experienced burnouts, thus, the test could not be continued. The reported values for  $\epsilon_{c,0.95}$  range from 0.37 - 0.42 % and,  $\epsilon_{irr,0.99}$  is 0.39 % for the samples.

### 3.3.3 Batch 3 Fabricated August 19, 2016

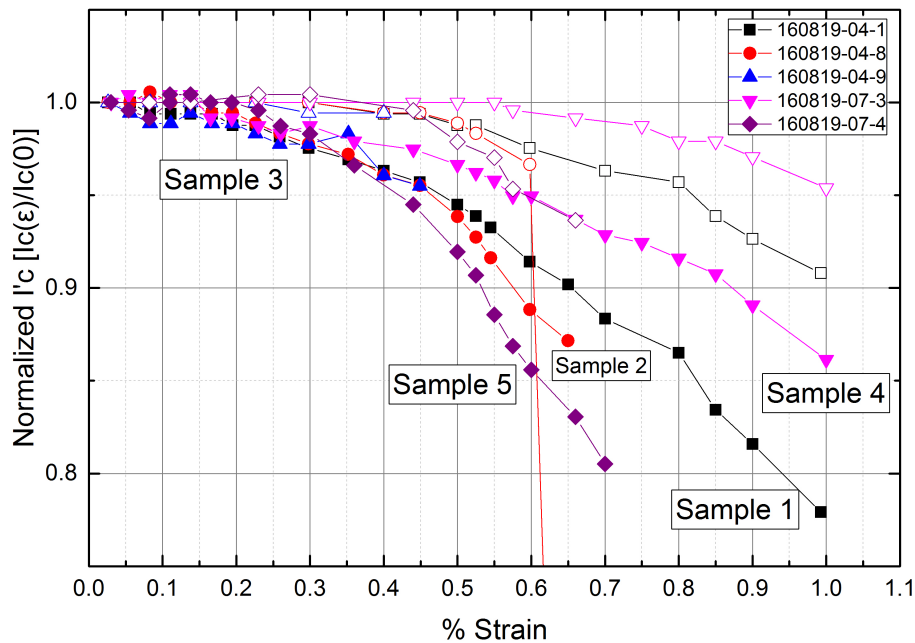


Figure 3.11: Normalized critical current vs. strain of SuNAM CC batch 3. Closed symbols represent the critical current while the sample is under load and open symbols show the critical current at the no-load condition after the strain was applied at 77 K.

Batch 3 had a total of five samples tested. Samples from this batch had been shown to be different mechanically, which suggested critical current vs. strain measurements would also differ. At 0.5 % strain the normalized  $I_c$  ranges from 0.86 % to about 0.95 % of the no-load  $I_c$  condition. Importantly, when each sample was returned to the no-load condition, the permanent damage was different for each sample. Sample 160819-07-3 (pink triangles) had the highest current retention at

0.58 % strain while sample 160819-07-4 (purple diamond) had the worst current retention at 0.41 % strain for  $\epsilon_{c,0.95}$ . For these set of samples the  $\epsilon_{c,0.95}$  range from 0.41-0.57 % and,  $\epsilon_{irr,0.99}$  ranged from 0.45-0.67 %.

# CHAPTER 4

## DISCUSSION

### 4.1 Stress-Strain Variability of SuNAM REBCO CC

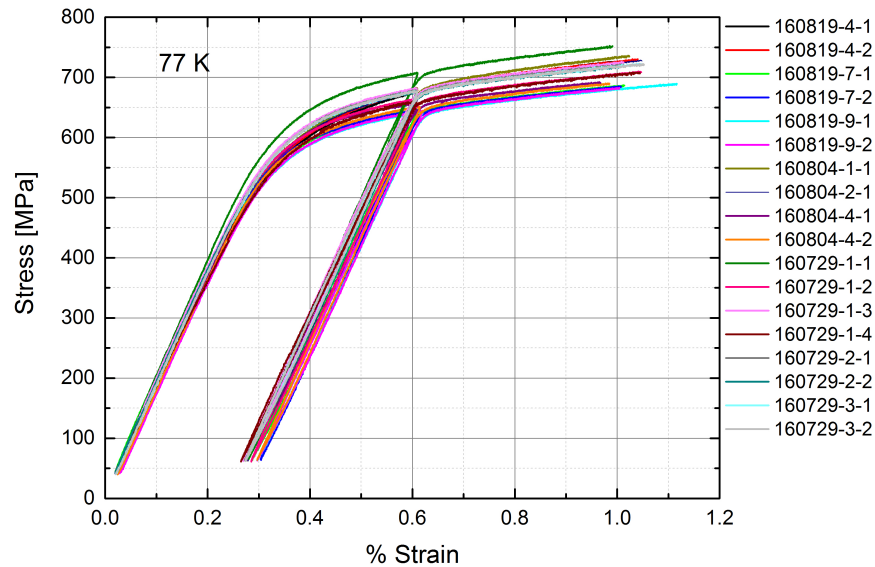


Figure 4.1: Stress vs. strain of 18 different SuNAM REBCO CC at 77 K, manufactured on August 19th, 2016 (160819), August 4th, 2016 (160804), and July 29th, 2016 (160729). I.e., 160819-4-1 represents manufactured date-spool number-sample number.

Figure 4.1 shows the results of 18 tensile tests for SuNAM REBCO CC measured at 77 K. Six samples from the manufacturing date of August 19th, 2016 (160819), four samples from August 4th, 2016 (160804), and eight samples from July 29th, 2016 (160729) were tensile tested. 0.2 % yield stress+ ( $\sigma_{0.2}$ ) ranged from 628-697 MPa with an average of 657 MPa and standard deviation of 17.6 MPa between all batches. The elastic modulus  $E$  of the SuNAM REBCO CC ranged from 181-187 GPa with an average of 184 GPa and standard deviation of 3.99 GPa.

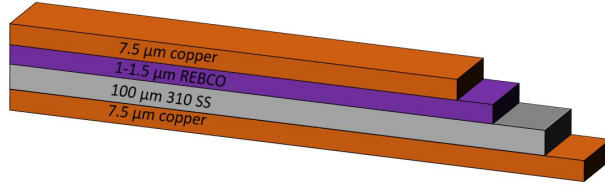


Figure 4.2: Thicknesses of layers in SuNAM REBCO CC (not to scale). Total copper thickness is 15  $\mu\text{m}$ , 1-1.5  $\mu\text{m}$  of REBCO, and 100  $\mu\text{m}$  of 310 SS.

All SuNAM REBCO CC tested had 100  $\mu\text{m}$  310 SS substrate, and 7.5  $\mu\text{m}$  of copper per side. Mechanical variability is clearly shown in Figure 4.1, even though all CCs should have the same area fractions of 310 SS and copper, seen in figure 4.2. The dominant component for the strength of SuNAM’s REBCO CC is the 100  $\mu\text{m}$  of 310 SS. The electroplated copper, while only being 13 % of the total volume fraction of the coated conductor, has a significant effect on the strength [9, 13].

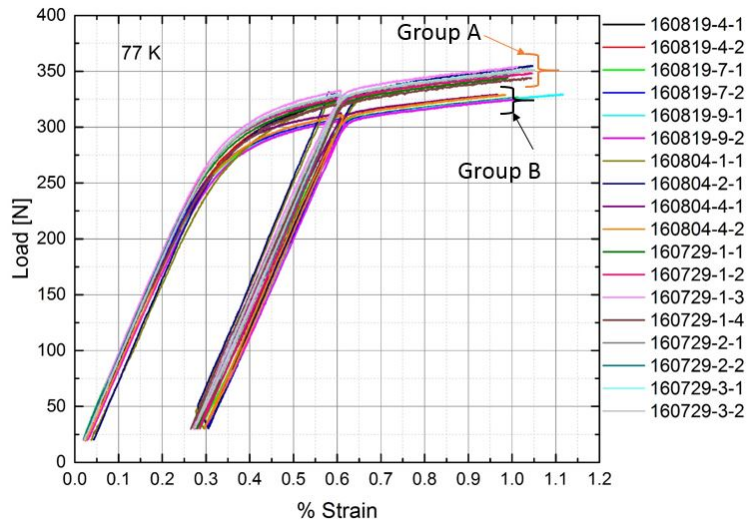


Figure 4.3: Load vs. strain of the 18 SuNAM REBCO CC samples. Group (A) and (B) show ”identical” conductors having different stiffnesses.

It was previously shown in Figure 4.1 that SuNAM REBCO CC had variability in its stress vs. strain curves. The extensometer used offers a resolution of  $\pm 2$  microstrain, thus ruling out its contribution to mismatch in the stress vs. strain curves. However, the engineering stress being a

function of the cross-sectional area would be the dominant factor in any mismatch produced in the experiment. Figure 4.3 shows the load vs. strain of the same 18 samples that were tensile tested. Two distinct groupings can be observed, namely, group A and B, suggesting that the source of variability is not solely from the cross-sectional area but perhaps due to the components of the coated conductor.

## 4.2 Annealing Effects on Hastelloy<sup>®</sup> and 310 SS Substrates

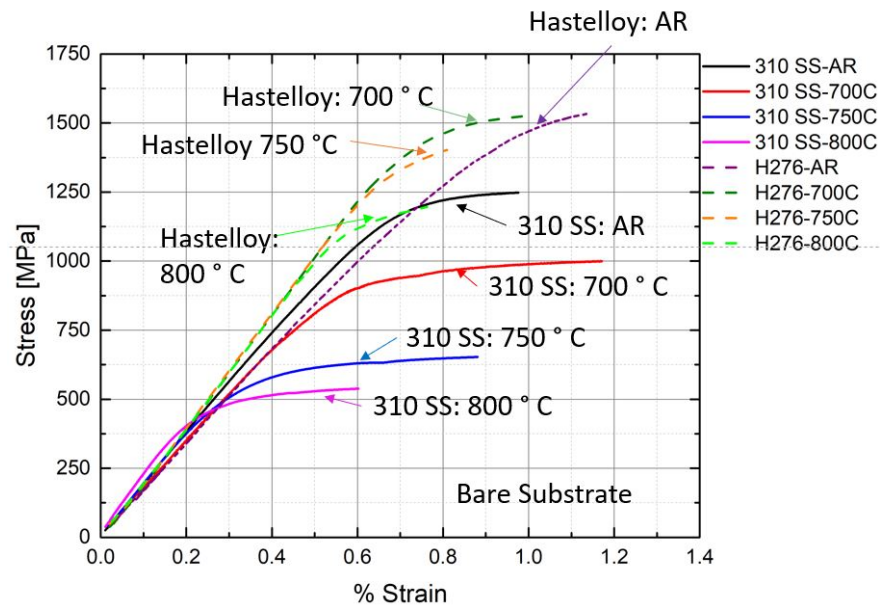


Figure 4.4: The average trend of as received and heat treated Hastelloy<sup>®</sup> C-276 and 310 SS bare substrate stress vs. strain curves at various conditions of heat treatments at AR(as received), 700°C, 750°C, and 800°C.

In Chapter 3, a comparison of the influence of simulated REBCO deposition treatment on bare Hastelloy<sup>®</sup> C-276 and 310 SS was shown. Figure 4.4 shows the average stress vs. strain trend of these varying heat treatment effects on the bare substrate strength. The 310 SS substrate became continuously weaker after each heat treatment while the Hastelloy<sup>®</sup> C-276 had increased mechanical properties until the 800°C heat treatment. The linear region of the 310 SS substrate after the 800°C heat treatment starts to become slightly non-linear, offering additional evidence of the sensitivity of the 310 SS to exact temperature during manufacturing.

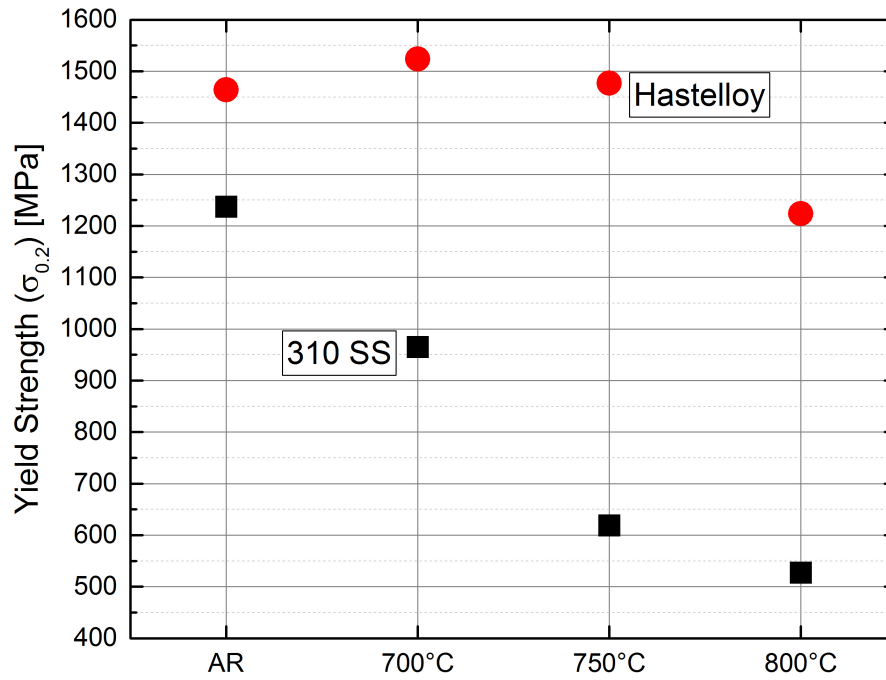


Figure 4.5: 0.2 % yield strength vs. heat treatment on Hastelloy<sup>®</sup> C-276 (red circle) and 310 SS (black square)

In Figure 4.5, the 0.2 % yield strength is plotted vs. the heat treatment. In the as received condition, there is a notable difference of yield strength between the Hastelloy<sup>®</sup> C-276 and 310 SS. This difference becomes increasingly apparent after each heat treatment. Hastelloy<sup>®</sup> C-276 interestingly increased its yield strength from ~ 1460 MPa to ~ 1520 MPa, while the 310 SS lowered its yield strength from ~ 1250 MPa to ~ 970 MPa after the 700°C heat treatment. Although exact deposition temperatures are not reported by either SuNAM or SuperPower, we estimate them to be in the 750-775°C range [4, 14]. Looking closer at the effect of 750°C heat treatment shows not much change in yield strength of the Hastelloy<sup>®</sup> C-276 while the 310 SS yield strength dropped considerably. A conclusion is the manufacturing with stainless steel is not ideal for REBCO CC as the strength is reduced during REBCO deposition.

### 4.3 $I_c$ -Strain Dependence of SuNAM REBCO CC

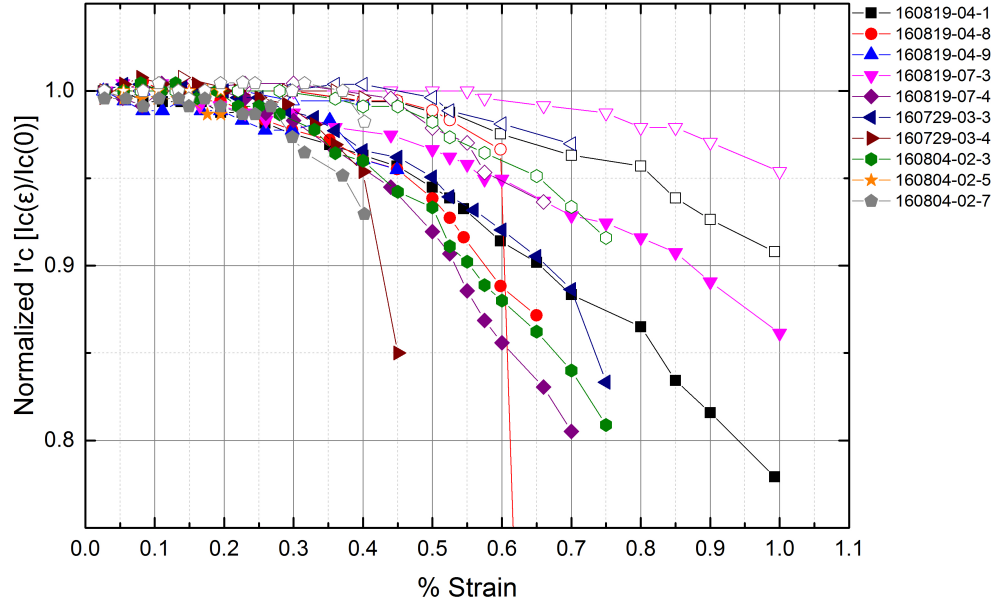


Figure 4.6:  $I_c$  vs. strain of SuNAM REBCO CC. Solid symbols indicate  $I'_c$  at strain, and open symbols indicate  $I'_c$  after the strain was applied. The red box show tests done with a one-inch Shepic extensometer to ensure extensometers can be used in  $I_c$  vs. strain tests.

Mechanically and electrically speaking, REBCO CC manufactured by SuNAM can be quite variable between batches. When all batches of the tested conductor are compared in Figure 4.6, a wide spread of current-carrying behavior was seen as the strain was applied. At present, high field magnet systems tend to be designed as to not apply more than 0.4 % strain on the conductor. What these results show is that this may not be sufficiently conservative since the normalized  $I_c$  ratio at 0.4 % strain does show  $I_c$  degradation, dropping the critical current to 95-96 % of the initial  $I_c$  value. After the degradation of  $I_c$  at 0.4 % strain, the normalized  $I_c$  returns back to 97-100 % of the initial  $I_c$  when the samples were in the “no strain” condition. That said, the electrical properties of the samples are different and do not all perform the same way. One theory for differences in electrical properties could be due to REBCO CC starting as 12 mm wide and then being slit to the desired size causing small cracks in the REBCO layer of the conductor.

### 4.3.1 Slit Edge Effects on $I_c$ vs. Strain

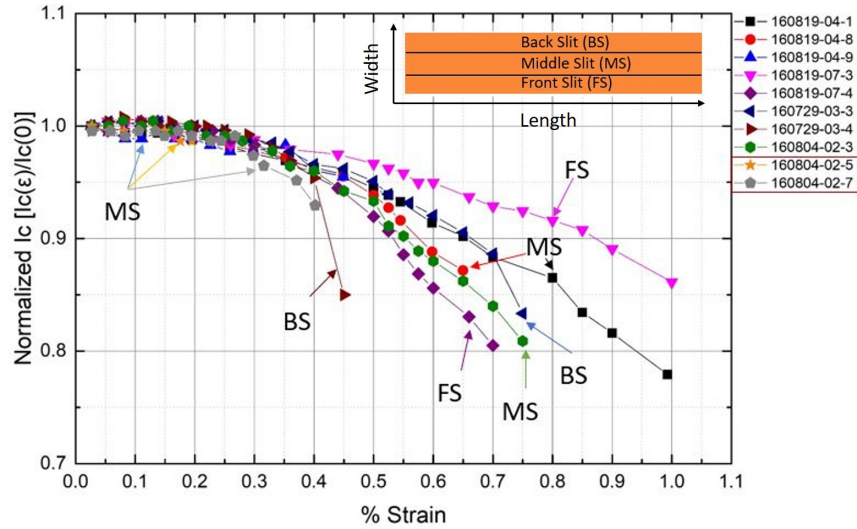


Figure 4.7:  $I_c$  vs. strain of SuNAM REBCO CC showing current dependence on strain. Labels indicate the type of slit edge on tested samples.

Differences in the current carrying capabilities of the REBCO CC was evident in the  $I_c$  vs. strain measurements. These differences could be from the placement of samples during slitting. Figure 4.7 shows the three types of slit placement experienced by the samples such as front slit (FS), back slit (BS), and the middle slit (MS). Slitting can cause cracks in the REBCO layer reducing the performance of the conductor; FS and BS tapes should have fewer cracks than MS tapes since they are slit on both sides. However, this appears not to be true due to some MS tapes handling higher strains than FS and BS tapes. No clear correlation can be made if the effects due to slitting affect the critical current dependence on strain.

### 4.3.2 Strain Gage Reinforcement Effect

An investigation of using strain gages to characterize REBCO CC was done during this study as another was to measure strain effects on critical current. A strain gage that is four millimeters wide was attached to a REBCO CC sample with strain gage glue. An extensometer is also attached underneath the strain gage as a way to check the accuracy of the strain gage. Figure 4.8 shows the

strain gage attached to the REBCO CC specimen. The possibility of reinforcement of the REBCO CC with strain gages was the primary motivation for this study.



Figure 4.8: REBCO CC with a mounted strain gage.

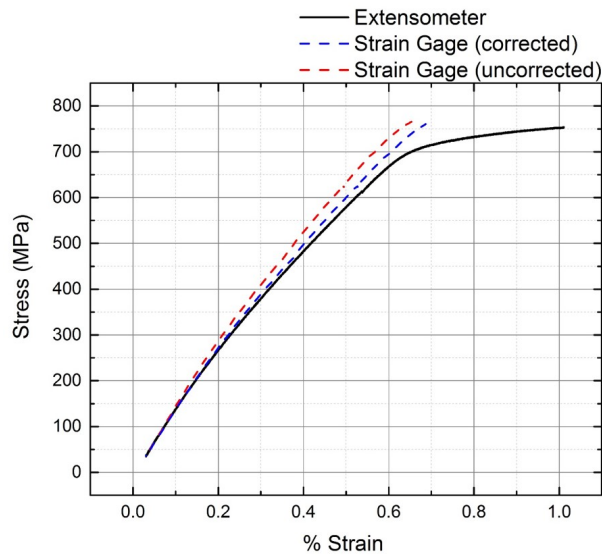


Figure 4.9: Strain gage reinforcement is shown in a tensile test with extensometer as a cross check. Red dash is reading directly from strain gage, blue dash line is corrected for reinforcement effect, and the solid line shows the results from the extensometer.

Figure 4.9 shows the results of the tensile test. The specimen was subjected to strain up to 1 %. The strain gage measured a strain of 0.63 % while the extensometer measured 1 % strain. we conclude that this mismatch is due to the reinforcement of the REBCO CC by the strain gage. Since the strain gage has approximately the same thickness as the specimen, the coated conductor is strengthened locally behind the strain gage. This effect can be accounted for by calculating an equivalent elastic modulus by using the thickness of the gage [15], which is about 0.079 mm with an elastic modulus of 13.8 GPa. The correction for the reinforcement is only accurate in the linear

elastic region of the conductor. Afterward, the strain gage becomes unreliable. We conclude that use of a strain gage is not recommended

# CHAPTER 5

## CONCLUSION

A number of high field magnets that utilize REBCO CC have proven to often be stress and strain limited. Due to the complex nature of copper plastically deforming and the high elastic modulus of 310 stainless steel and Hastelloy<sup>®</sup> which generally, operates in the elastic region, it is still uncertain how to accurately predict safe operating stresses and strain. Magnet designers often implement a strain limit of 0.4 % in newer magnet designs but this work shows that SuNAM tapes become partially plastic at the 0.4-0.5 % strain limit. On the other hand, SuperPower REBCO tapes are still in the linear elastic region if a low copper fraction is used. The main difference between the SuNAM and SuperPower REBCO CC is the type of substrate used between them. Clearly cold-rolled Hastelloy<sup>®</sup> C276 is much stronger than cold rolled 310 SS after deposition.

Mechanical variability is quite apparent in the SuNAM REBCO CC, most likely due to the heating during the REBCO deposition process. Since the manufacturing process SuNAM uses evaporates the buffer and REBCO layer continuously on the 310 stainless steel substrate, variable annealing occurs affecting the mechanical properties of the REBCO CC.

This study of simulating the vapor deposition process with heat treatments shows there is a strong link between temperatures used for deposition and the properties of the 310 stainless steel. By contrast, Hastelloy<sup>®</sup> was only weakly affected by the REBCO deposition heat treatment. This provides strong evidence that using Hastelloy<sup>®</sup> as the substrate is a better option than the 310 stainless steel.

Future work for the continuation of this study should include how the microstructure of the bare substrates change with the short heat treatments.  $I_c$ -strain tests revealed that the conductor's current carrying capacity degrades at different rates even when the same batch of conductor is used. Pre-existing cracks in the REBCO layer from slitting of the tape should be further examined as the cracks could be propagating at different rates.

# APPENDIX A

## DIMENSIONS OF MEASURED SAMPLES

### A.1 Dimensions of SuNAM REBCO CC

Table A.1: Dimensions of SuNAM REBCO CC Batch 1

Batch No.	Batch Subset	Tensile Spec No	Thickness (outside-inside-outside)			Width mm
			mm			
Batch 1	-01	1	0.119	0.119	0.120	4.05
			0.120	0.120	0.120	4.05
			0.122	0.121	0.122	4.06
	-01	2	0.123	0.122	0.123	4.05
			0.121	0.121	0.121	4.05
			0.119	0.120	0.120	4.06
	-01	3	0.122	0.121	0.122	4.06
			0.120	0.120	0.121	4.06
			0.119	0.119	0.120	4.05
	-01	4	0.119	0.120	0.119	4.04
			0.120	0.119	0.120	4.04
			0.121	0.121	0.122	4.05
	-02	1	0.121	0.121	0.121	4.04
			0.119	0.120	0.119	4.05
			0.118	0.118	0.119	4.06
	-02	2	0.119	0.118	0.119	4.04
			0.120	0.119	0.120	4.05
			0.122	0.121	0.122	4.05
	-03	1	0.119	0.119	0.118	4.06
			0.119	0.120	0.119	4.06
0.122			0.122	0.122	4.06	
-03	3	0.119	0.118	0.120	4.02	
		0.119	0.120	0.119	4.03	
		0.121	0.121	0.122	4.03	
-03	4	0.122	0.121	0.122	3.97	
		0.120	0.119	0.120	3.98	
		0.119	0.12	0.119	3.99	

Table A.2: Dimensions of SuNAM REBCO CC Batch 2

Batch No.	Batch Subset	Tensile Spec No	Thickness (outside-inside-outside)			Width
			mm	mm	mm	mm
Batch 2	-01	1	0.121	0.122	0.122	3.99
			0.120	0.120	0.119	3.99
			0.120	0.119	0.119	3.98
	-01	2	0.122	0.121	0.121	4.04
			0.120	0.119	0.120	4.04
			0.123	0.123	0.123	4.04
	-02	2	0.117	0.117	0.118	3.96
			0.120	0.120	0.120	3.96
			0.122	0.123	0.123	3.97
	-04	1	0.122	0.121	0.121	4.05
			0.120	0.120	0.120	4.05
			0.121	0.119	0.120	4.05
	-04	2	0.122	0.123	0.123	3.97
			0.120	0.121	0.120	3.98
			0.118	0.117	0.117	3.97

Table A.3: Dimensions of SuNAM REBCO CC Batch 3

Batch No.	Batch Subset	Tensile Spec No	Thickness			Width
			(outside-inside-outside)			
			mm			
Batch 3	-04	1	0.119	0.117	0.118	4.03
			0.119	0.119	0.119	4.02
			0.123	0.121	0.122	4.03
	-04	2	0.122	0.123	0.121	4.02
			0.119	0.118	0.118	4.03
			0.119	0.118	0.119	4.03
	-04	10	0.119	0.118	0.118	4.03
			0.120	0.120	0.119	4.04
			0.121	0.121	0.122	4.03
	-07	1	0.118	0.118	0.117	3.98
			0.118	0.120	0.119	3.97
			0.122	0.122	0.123	3.97
	-07	2	0.118	0.117	0.118	3.97
			0.120	0.119	0.120	3.96
			0.122	0.123	0.122	3.97
	-09	1	0.118	0.122	0.118	3.97
			0.118	0.120	0.121	3.96
			0.122	0.123	0.123	3.97
	-09	2	0.118	0.117	0.118	3.98
			0.121	0.120	0.120	3.99
			0.123	0.123	0.122	3.98

## REFERENCES

- [1] M. K. Wu, J. R. Ashburn, C. J. Torng, P. H. Hor, R. L. Meng, L. Gao, Z. J. Huang, Y. Q. Wang, and C. W. Chu, "Superconductivity at 93 K in a new mixed-phase y-Ba-Cu-O compound system at ambient pressure," *Phys. Rev. Lett.*, vol. 58, pp. 908–910, Mar 1987.
- [2] SuNAM Co. LTD., "Reactive co-evaporation by deposition & reaction," 2009. [Online]. Available: [http://i-sunam.com/home/en\\_technology,1,2,1,1](http://i-sunam.com/home/en_technology,1,2,1,1)
- [3] SuperPower Inc., "2g hts wire," 2009. [Online]. Available: <http://www.superpower-inc.com/content/2g-hts-wire>
- [4] S. Gnanarajan and N. Savvides, "Dual ion beam assisted magnetron deposition of biaxially textured ysz and ybco/ysz thin films," *Surface and Coatings Technology*, vol. 305, pp. 116 – 122, 2016.
- [5] D. G. R. William D. Callister, *Materials Science and Engineering: An Introduction, 8th Edition*. Wiley, 2009.
- [6] "ASTM e1450-16, standard test method for tension testing of structural alloys in liquid helium." [Online]. Available: <http://www.astm.org/cgi-bin/resolver.cgi?E1450-16>
- [7] "ASTM e111-17, standard test method for young's modulus, tangent modulus, and chord modulus." [Online]. Available: <http://www.astm.org/cgi-bin/resolver.cgi?E111-17>
- [8] "ASTM e8 / e8m-16a, standard test methods for tension testing of metallic materials, astm international." [Online]. Available: <http://www.astm.org/cgi-bin/resolver.cgi?E8E8M-16a>
- [9] Y. Zhang, D. W. Hazelton, R. Kelley, M. Kasahara, R. Nakasaki, H. Sakamoto, and A. Polyanski, "Stress-strain relationship, critical strain (stress) and irreversible strain (stress) of ibad-mocvd-based 2G HTS wires under uniaxial tension," *IEEE Transactions on Applied Superconductivity*, vol. 26, no. 4, pp. 1–6, June 2016.
- [10] Micro-Measurements, "Strain Gages & Load Cells types and specifications of strain gages," 2018. [Online]. Available: <http://www.vishaypg.com/docs/11055/tn505.pdf>
- [11] K. Gramoll, "MECHANICS-THEORY: Strain Gage Theory." [Online]. Available: [https://www.ecourses.ou.edu/cgi-bin/ebook.cgi?doc=&topic=me&chap\\_sec=08.3&page=theory](https://www.ecourses.ou.edu/cgi-bin/ebook.cgi?doc=&topic=me&chap_sec=08.3&page=theory)
- [12] R. B. Leonard, "Thermal stability of hastelloy alloy c-276," *CORROSION*, vol. 25, no. 5, pp. 222–232, 1969. [Online]. Available: <https://doi.org/10.5006/0010-9312-25.5.222>

- [13] R. P. Walsh, D. McRae, W. D. Markiewicz, J. Lu, and V. J. Toplosky, “The 77-K stress and strain dependence of the critical current of ybco coated conductors and lap joints,” *IEEE Transactions on Applied Superconductivity*, vol. 22, no. 1, pp. 8 400 406–8 400 406, Feb 2012.
- [14] X.-Y. Zheng, D. H. Lowndes, S. Zhu, J. D. Budai, and R. J. Warmack, “Early stages of  $\text{YBa}_2\text{Cu}_3\text{O}_{7-\delta}$  epitaxial growth on  $\text{MgO}$  and  $\text{SrTiO}_3$ ,” *Phys. Rev. B*, vol. 45, pp. 7584–7587, Apr 1992. [Online]. Available: <https://link.aps.org/doi/10.1103/PhysRevB.45.7584>
- [15] A. Ajovalasit, S. Fragapane, and B. Zuccarello, “The reinforcement effect of strain gauges embedded in low modulus materials,” *Strain*, vol. 49, no. 4, pp. 366–376. [Online]. Available: <https://onlinelibrary.wiley.com/doi/abs/10.1111/str.12043>

## BIOGRAPHICAL SKETCH

Kyle Radcliff is a graduating master's student in mechanical engineering at Florida State University. Kyle was born in Hollywood, FL on August 5th 1993 and is the second oldest of three children. He graduated high school from Hollywood Hills High in 2011 and became the second member in his family to go to college. In 2013, he became the captain of the Society of Automotive Engineers Baja race team. He broke the previous record of highest overall competition placement by placing 43rd out of 120 teams. In his senior year of undergraduate study, he pursued interest in superconducting magnet research under Dr. Seungyong Hahn. In 2016, he graduated with his bachelors degree in mechanical engineering and pursued his master's under the supervision of Dr. Hahn. He is now the first in his family to obtain a master's degree.